VOLUME 23, 1961/62, No. 10 pp. 293-324 Published 25th. July 1962

Philips Technical Review

DEALING WITH TECHNICAL PROBLEMS
RELATING TO THE PRODUCTS, PROCESSES AND INVESTIGATIONS OF
THE PHILIPS INDUSTRIES

STANDARD NOISE SOURCES

by P. A. H. HART *).

621.391.822.3:621.385.2

A standard noise source can be a resistor, a saturated diode or a gas discharge. These three types are dealt with in the article below, and it is shown which type is to be preferred in the various frequency ranges. Some standard noise sources specially designed in the Philips Laboratories are discussed.

Introduction

If signals are to be made perceptible — we are concerned here primarily with radio and radar signals — the signal strength must exceed a certain minimum, irrespective of the amplification of the receiving system. The reason for this is the presence of noise. The minimum referred to depends on the particular technique of "information processing" used, and is low in some special techniques such as single-sideband systems and the methods used in radio astronomy.

The noise comes from sources that can be divided into two categories. The first comprises the *external* sources. It is these that cause the receiving aerial to pick up noise in addition to the desired signal. External kinds of noise include atmospherics, thermal noise from the earth and cosmic noise.

The second category comprises the *internal* sources of noise, inside the receiver itself. Their contribution makes the signal-to-noise ratio at the output of the receiver worse than at the input. The noise added by internal sources can be minimized by careful circuitry and the suitable choice of components, but it cannot be entirely eliminated; some noise from resistors, valves and other circuit elements always remains.

The strength of the internal noise is usually measured in a relatively narrow band of frequencies; the average frequency of this band is called "the" frequency at which the noise is measured. The measurement can be made by comparison with a known noise power delivered by a *standard noise source*. There are various types of standard noise source. Which type is used depends among other things on the frequency at which the measurement is to be made.

A standard noise source that delivers an accurately known noise power is a *resistor of known resistance and temperature*. Requiring no calibration, this noise source is an *absolute* standard.

It is often more convenient to use a *noise diode*, i.e. a diode operated at the saturation current. Because of the shot effect the current fluctuates. A noise diode is a *noise-current generator*. The value of the noise current can be calculated from the direct current flowing in the diode; the noise diode too is therefore an absolute standard, but only in a limited (though wide) range of frequencies. As will presently be shown, this range has both a lower and an upper limit.

At frequencies higher than those at which the noise diode is effective, use can be made of a *gas-discharge noise source*. Noise generators of this type are sub-standards, in the sense that the noise power delivered cannot be exactly calculated but must be determined by calibration. They can be made with highly stable characteristics and are relatively insensitive to fluctuations in supply voltage and ambient temperature. For these reasons it is not necessary to calibrate them individually, unless

*) Philips Research Laboratories, Eindhoven.

extreme precision is required, as for instance in radio-astronomic measurements. Compared with a resistor, gas-discharge noise sources deliver a high noise power. Various designs are possible. As we shall see, in decimetre-wave equipment the gas discharge is coupled to a helix or a Lecher line, and in equipment operating on centimetre or millimetre wavelengths the discharge tube is mounted in a waveguide. In other designs the gas discharge is in a resonant cavity or in a horn antenna.

Fig. 1 gives a broad indication of the operating ranges of the Philips noise diodes K 81A and 10 P, and of gas-discharge tubes of varying constructions; the boundaries are in fact not as sharp as are shown here.

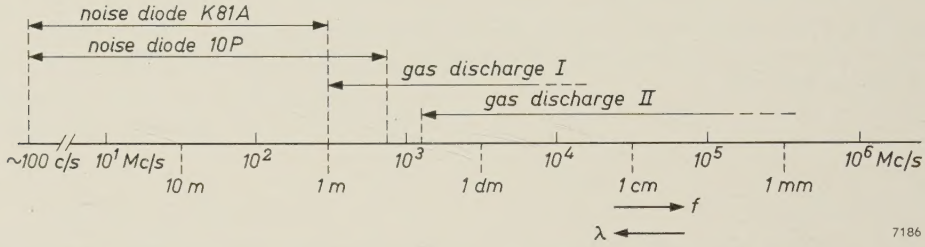

Fig. 1. Rough indication of the frequency and wavelength ranges in which noise diodes and gas discharges can be used as standard noise sources. *Gas discharge I* relates to a discharge tube coupled to a helix (fig. 17*a*), *gas discharge II* to a discharge tube mounted in a waveguide (fig. 17*b* and *c*).

In this article the three main types of noise source — resistor, diode and gas-discharge — will be discussed. We shall consider some special designs, the corrections necessary in certain applications of the noise diode, and gas-discharge noise sources for various wave ranges, including the millimetre band.

The resistor as a noise source

The thermal noise of a resistance R in a relatively narrow frequency band Δf around the frequency f is given by Nyquist's noise theorem:

$$\overline{u^2} = \frac{4hf}{e^{hf/kT} - 1} R \, \Delta f . \quad . . . \quad (1)$$

Here $\overline{u^2}$ is the mean square noise voltage, k is Boltzmann's constant ($= 1.38 \times 10^{-23}$ joule/°K), T is the absolute temperature of the resistor, and h is Planck's constant ($= 6.6 \times 10^{-34}$ joule-second). If hf is small compared with kT, i.e. if

$$f \ll \frac{k}{h} T \approx 2 \times 10^{10} T \text{ c/s} ,$$

formula (1) can be simplified to

$$\overline{u^2} = 4 k T R \, \Delta f . \quad . . . . \quad (2)$$

Measurement of the noise factor with standard noise resistors

An example of the use of resistors as standard noise sources is the measurement of the noise factor of a circuit, an amplifier for instance, that can be treated as a linear four-terminal network.

The noise factor F as defined by the American standard (53 I.R.E. 7 S1) is [1]):

$$F = \frac{N_0 + N_{\text{extra}}}{N_0} . \quad . . . \quad (3)$$

Here $N_0 + N_{\text{extra}}$ is the total noise power at the output in the narrow frequency band Δf, and N_0 is the share contributed by the thermal noise of an impedance Z_i which is connected externally across the input terminals and is equal to the impedance of the signal source to which the four-terminal network is normally connected (e.g. an antenna); the temperature of Z_i must be 290 °K. Therefore N_{extra} is the portion of the output noise added by the four-terminal network [2]).

The noise factor is determined by measuring the output noise power (still in the narrow band Δf) when Z_i is successively at the temperatures T_1 and T_2, which must be known; see *fig. 2*. If only the temperature of Z_i were to change between the two measurements (Z_i itself thus remaining constant) the output noise power when Z_i has the temperature T_1 would be:

$$P_1 = CT_1 + N_{\text{extra}} ,$$

and when Z_i has the temperature T_2:

$$P_2 = CT_2 + N_{\text{extra}} .$$

[1]) See also F. L. H. M. Stumpers and N. van Hurck, An automatic noise figure indicator, Philips tech. Rev. **18**, 141-144, 1956/57.

[2]) It would be going too far to deal here with the way in which the noise factor as defined depends on Z_i. In this connection reference may be made to A. G. T. Becking, H. Groendijk and K. S. Knol, The noise factor of four-terminal networks, Philips Res. Repts **10**, 349-357, 1955.

In these two expressions C is a constant. Let the temperature 290 °K, mentioned in the definition, be denoted by T_0; then $N_0 = CT_0$. If we put $P_2/P_1 = a$, it follows from (3) that:

$$F = \frac{\frac{T_2}{T_0} + a - 1 - a\frac{T_1}{T_0}}{a-1}. \quad \ldots \quad (4)$$

For $T_1 = T_0$ this reduces to

$$F = \frac{\frac{T_2}{T_0} - 1}{a-1}. \quad \ldots \quad (5)$$

The latter expression is still valid to a good approximation when the difference between T_1 and T_0 is small.

In accordance with the definition of the noise factor we have spoken above of an *impedance* Z_i. Every impedance can be treated as composed of a resistance and a reactance connected in parallel (or in series). As the reactance causes no noise and is not changed during the measurement, it can be regarded as belonging to the four-terminal network. The noise-factor measurement therefore amounts to determining the ratio a of the output noise powers when a *resistor* R of temperature T_1 ($\approx T_0$) and T_2 respectively is connected across the input.

Measurements using a resistor as standard noise source are in principle possible at any frequency. In the range of ultra-high frequencies (decimetre wavelengths and shorter) a resistor is in fact the only absolute standard noise source. Nevertheless, in all frequency ranges — with the sole exception of the audio frequencies [3]) — the resistor has been superseded as a noise source for routine measurements by the noise diode or the gas discharge. The reasons are of a practical nature:

1) To bring a resistor to the temperature T_2, an oven or a temperature bath is needed, which is a complication.
2) An error is caused by the fact that the resistance changes as a rule with temperature. Two resistors are therefore needed, one of which must have the same resistance at the temperature T_1 as the other at the temperature T_2, which is much higher or lower than T_1.
3) If T_2 is higher than T_1, the temperature difference $T_2 - T_1$ cannot be made very large without damaging the hot resistor. The highest temperature can be achieved with a tungsten filament ($T_2 = 2700$ °K); $T_2 - T_1$ is then about 2400 °K. This means that large noise factors cannot be accurately measured with a hot resistor: N_{extra} is then large compared with CT_1 and CT_2, and therefore $P_2 \approx P_1$, i.e. $a \approx 1$, so that $a - 1$ cannot be determined with great precision.

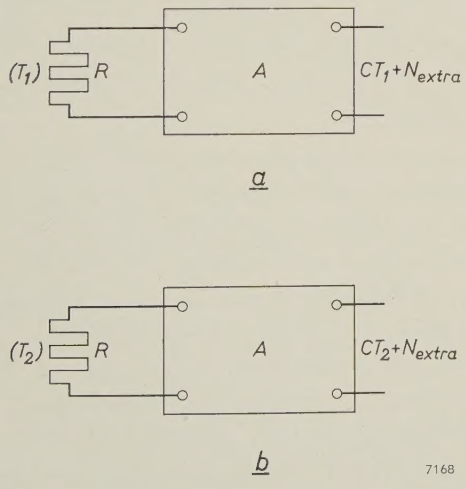

Fig. 2. Measurement of the noise factor of a four-terminal network A by means of standard noise resistors. *a*) Connected to the input terminals of A is a resistance R having the temperature T_1. *b*) A resistor R is again connected to the input terminals, but now has the temperature T_2. The noise factor can be calculated from the measured values of the output noise in a narrow frequency band Δf.

Apart from its use at audio frequencies, the resistor as a noise source is now mainly used for *calibrating* noise diodes in the decimetre bands and gas-discharge tubes in the centimetre and millimetre bands. An example will be given at the end of this article.

Special designs of resistors as standard noise sources

In noise measurements at very short waves the stray inductance and capacitance of conventional resistors cause an impermissible error. Special resistors are therefore needed, and we shall describe here two that have been designed and constructed in the Philips Research Laboratories at Eindhoven. One serves for calibrating noise diodes in the decimetre bands and is a *cold* resistor ($T_2 = 77$ °K) [4]); the other is used for calibrating gas discharges in the centimetre and millimetre bands, and is a *hot* resistor ($T_2 = 1336$ °K).

a) A cold resistor for decimetre waves

The resistor proper (*fig. 3*) consists of a very thin layer of platinum on a hard-glass tube, located at the end of an impedance transformer fitted with shorting plungers. The layer has a resistance of roughly 50 ohm. The resistance, as "seen" from the input of the impedance transformer, is accurately set to 50 ohm by adjusting the plungers until a standing-wave detector, having a 50-ohm characteristic

[3]) See e.g. A. van der Ziel, Noise, Prentice Hall, New York 1954, p. 31.

[4]) Another cold resistor is described in Philips tech. Rev. **21**, 327 (fig. 13), 1959/60.

impedance, gives a standing-wave ratio of 1. Both the resistor itself and the impedance transformer are immersed in liquid nitrogen (temperature 77 °K). As regards its noise contribution, therefore, the dissipative resistance of the transformer also behaves as a resistor having a temperature of 77 °K. *Fig. 4* shows a photograph of the transformer with the resistor inside.

The second resistor in the measurement can be a conventional type of 50 ohm, kept at room temperature.

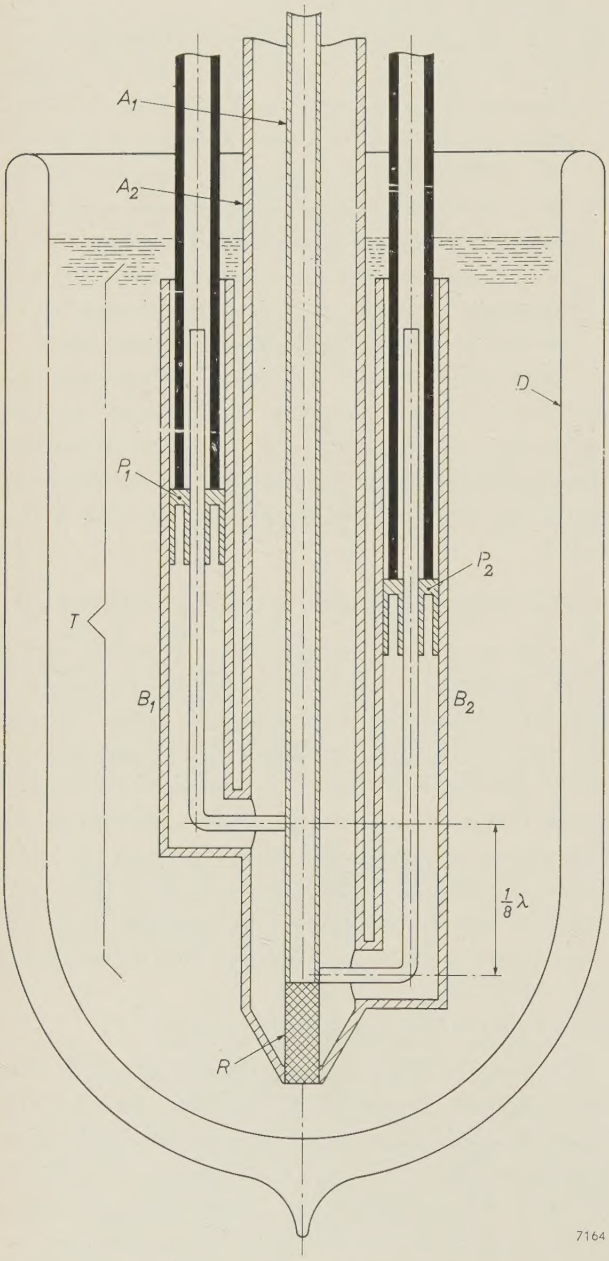

Fig. 3. Construction of a cold standard noise resistor for decimetre waves (not to scale). R is the actual resistor (approx. 50 ohm), being a layer of platinum on glass. T coaxial impedance transformer consisting of an inner conductor A_1 and an outer conductor A_2 with coaxial side branches B_1 and B_2, which are terminated by shorting plungers P_1 and P_2. At the top a coaxial plug (N plug) can be connected. D Dewar vessel filled with liquid nitrogen (temperature $T_2 = 77$ °K).

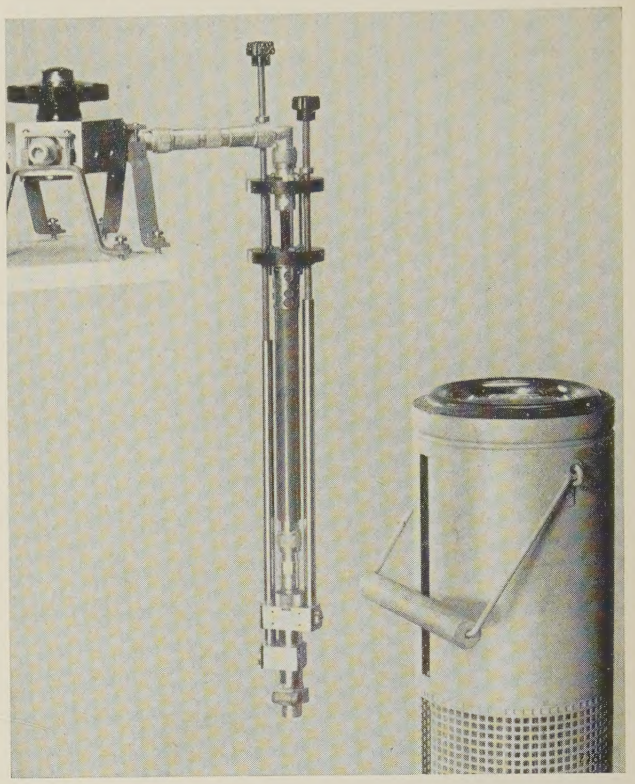

Fig. 4. The impedance transformer represented in fig. 3 (with the noise resistor inside) removed from the nitrogen bath.

b) A hot "resistor" for centimetre and millimetre waves

A waveguide (*fig. 5*) is provided with a matched termination at one end in the form of an absorption wedge, made in this case of the ceramic material "Caslode". The part of the waveguide with the wedge is uniformly heated in an oven to a well-defined high temperature. The temperature is measured with a thermocouple or a pyrometer, which need only be calibrated for this one temperature — which has been chosen as the melting point of gold (1336 °K) [5].

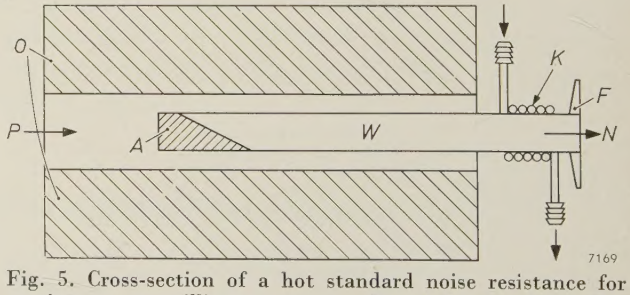

Fig. 5. Cross-section of a hot standard noise resistance for centimetre or millimetre waves. W platinum waveguide. A absorption wedge (the noise source proper). F connecting flange. O electric oven. K pipe carrying cooling water. Arrow N indicates the direction in which the noise leaves the waveguide, arrow P the direction in which the optical pyrometer faces; the latter measures the temperature T_2 of the wedge A.

[5]) The method of calibration has been described in: K. S. Knol, A thermal noise standard for microwaves, Philips Res. Repts **12**, 123-126, 1957.

To prevent oxidation, the waveguide is made of (thin) platinum. The part outside the oven is water-cooled to avoid overheating the coupling flange and the components connected to it. *Fig. 6* shows waveguides of this type for wavelengths of 3 cm and 8 mm.

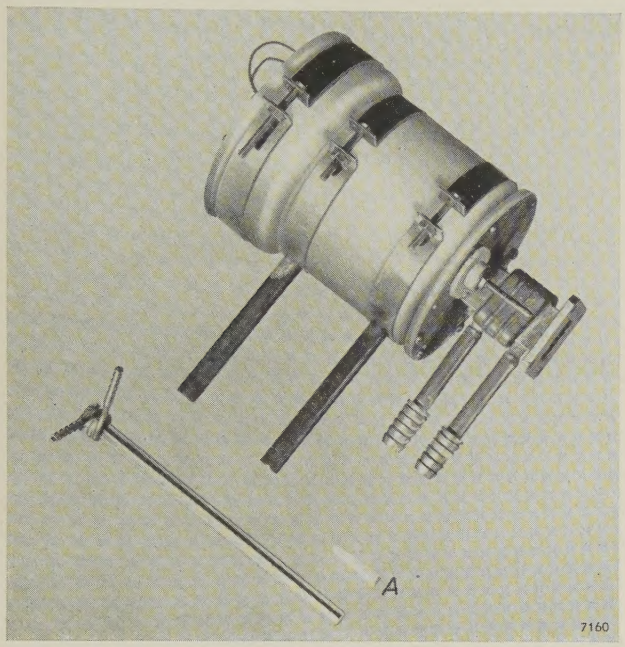

Fig. 6. Hot standard noise sources as in fig. 5, for wavelengths of 3 cm (with oven) and 8 mm (without oven). At *A* can be seen the "Caslode" absorption wedge for the 8 mm waveguide.

The second waveguide used in the measurement contains a matched termination made of wood, at room temperature.

Before concluding this account of standard noise resistors, there are two further points to be noted. One concerns the choice between cold and hot resistors, the other a correction required in certain cases.

We have just discussed a cold resistor for decimetre waves and a hot resistor for centimetre and millimetre waves. In principle the converse is also possible. Compared with a cold resistor a hot resistor has the advantage of delivering a higher noise power, which can increase the accuracy of the measurement (unless the noise figure is low). This is an argument in favour of choosing a hot resistor. Decimetre-wave techniques using Lecher wires or coaxial lines are not so suitable at high temperatures, however, as microwave techniques using waveguides. For this technological reason we decided on a cold resistor for the decimetre bands.

The standard noise resistor which is at the high or low temperature T_2 gives rise to a temperature gradient in the supply line (coaxial cable or waveguide). This must be taken into account in two respects. Firstly, the materials employed must be capable of withstanding the temperature gradient. Secondly, the calculated value of the noise generated by the resistor R needs to be corrected if the losses in the supply line are at all significant (e.g. a few percents of those in R), for part of the noise produced by R is lost in the dissipative resistance of the supply line, whilst the latter resistance itself contributes a certain amount of noise.

The diode as a noise source

A diode operated at saturation behaves in a wide range of frequencies like a noise-current generator having an infinite internal resistance. In a relatively narrow band Δf within that range the mean square noise current is given by Schottky's formula:

$$\overline{i^2} = 2\,qI_s\Delta f, \qquad \ldots\ldots \quad (6)$$

where q is the charge on the electron ($= 1.60 \times 10^{-19}$ C) and I_s is the saturation current flowing in the diode. I_s depends on the temperature of the filament and therefore the noise current can be given a different value by changing the filament current.

The usual practice for measurements is to connect the noise diode in parallel with a resistor R (*fig. 7a*). In fig. 7*b* the diode is represented by a noise-current source I, and the resistance R by an equal but hypothetically noiseless resistance R^* in series with a noise-voltage source U which accounts for the thermal noise of R. In addition to this thermal noise, given by $4kT_1R\Delta f$ (T_1 being the temperature of R), the resistance R in fig. 7*a* carries the noise voltage generated by the noise current of the diode; this noise is given by $2qI_sR\Delta f$. Since the two noise sources are independent of each other, the total noise is found by simply adding the two contributions mentioned. We now want to find the temperature T_{eq} which a resistor R must have if its thermal noise is to be equal to this total:

$$4\,kT_{eq}R\Delta f = 4kT_1R\Delta f + 2qI_sR^2\Delta f\,.$$

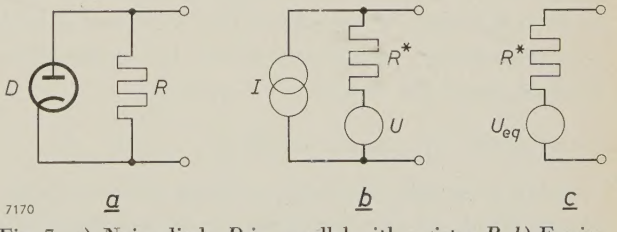

Fig. 7. *a*) Noise diode D in parallel with resistor R. *b*) Equivalent circuit of (*a*) consisting of a noise-current source I, representing the diode noise, shunted across a noiseless resistor R^* which is in series with the noise-voltage source U representing the noise from R. *c*) Equivalent circuit of (*b*) — likewise of (*a*) — consisting of a noiseless resistor R^* in series with a noise-voltage source U_{eq} which delivers the same noise as a resistor R at the temperature T_{eq}.

We can solve this expression for T_{eq}:

$$T_{eq} = \frac{q}{2k} I_s R + T_1 .$$

Insertion of the numerical values of q and k gives $q/2k = 5800$ °K/V $= 20 \times 290$ °K/V $= 20\ T_0$ °K/V, so that the formula for T_{eq} can also be written:

$$T_{eq} = 20\ I_s R T_0 + T_1. \quad . \ . \ . \ . \ . \quad (7)$$

A noise diode in parallel with a resistor R (fig. 7*a*) thus constitutes a noise source which is equivalent to a resistor R at the temperature T_{eq} (represented in fig. 7*c* as a noiseless resistor R^* in series with a noise-voltage source U_{eq}); as can be seen from eq. (7), T_{eq} can be varied by changing the current I_s by means of the filament current of the diode.

Determining the noise factor with a noise diode

The noise factor of a four-terminal network can be determined with a noise diode as follows. The diode with a resistor in parallel is connected to the input terminals of the network, and the noise power P_1 is measured at the output, in the small frequency band Δf, with the diode passing no current; the noise power P_2 is then measured with the diode in operation. Again putting $P_2/P_1 = a$, we find from the definition of the noise factor, using (6) and (7):

$$F = \frac{20\ I_s R - 1 + a + (1 - a)\dfrac{T_1}{T_0}}{a - 1} . \quad (8)$$

This formula is very much simpler if the temperature T_1 of the resistor is roughly equal to T_0 (= 290 °K) and if a is given the value 2 (i.e. if the diode current I_s is adjusted so that $P_2 = 2P_1$; see [1])). In that case:

$$F = 20\ I_s R . \quad . \ . \ . \ . \ . \ . \quad (9)$$

Formulae (8) and (9) are valid in a wide frequency range. In this range the diode is an absolute noise standard, since the formulae contain no empirical constants. We shall now consider the limits of this frequency range. We shall see that they are partly of a fundamental nature and partly due to the finite dimensions of the diode.

Lower limit of frequency range

Below a certain frequency a diode shows in addition to the above-mentioned noise, which is due to the shot effect, a kind of noise known as flicker noise [6]). According to one theory, flicker noise is bound up with the "scintillating" character of the emission: after a certain spot on the cathode has emitted a batch of electrons, some time elapses before the same spot can emit electrons again. Investigations have shown [7]) that a tungsten cathode, as used in noise diodes, exhibits distinct flicker noise only at frequencies of 10 c/s and lower. Impurities in the cathode and traces of gas may raise this limit, however, so that it is safer not to use a diode for noise measurements below, say, 100 or 1000 c/s.

In practice, this limitation is of little significance, noise diodes seldom being used in the audio-frequency range. Noise measurements at audio frequencies are usually done with two different resistors, both at room temperature [8]).

Upper limit of frequency range

At very high frequencies there are two causes of deviations from the Schottky formula (eq. 6): one we shall call the "transformation error" and the other the "transit-time error". The transformation error is attributable to stray capacitances and inductances; the transit-time error is significant at frequencies which are so high that the period of oscillation is not long compared to the time taken by the electrons to travel from cathode to anode. We shall now consider the magnitude of these errors.

The transformation error

Some years ago a short article appeared in this journal [9]) describing a new noise diode (the 10 P type already mentioned) and two circuits making use of this diode for noise measurements in the decimetre wave range; one circuit employed a Lecher system and the other a coaxial system (*fig. 8a*). To calculate the transformation error of such a circuit, we use the equivalent circuit shown in *fig. 9a*. Here the current source i represents the noise diode, C_0 the capacitance of the diode, L_0 the inductance of the lead-in wires, Z_1 the impedance of the coupling capacitors, and Z the resistance R and the section of transmission line connected in parallel with it. The other end of this line is fitted with a shorting plunger, which is so adjusted that, at the operating frequency f, the impedance Z is equal to R (i.e. such that the shorted section of line exactly compensates the influence of the various reactances at this frequency). To examine the influence of L_0, C_0 and Z_1 on the noise, we transform this circuit into one in which Z is shunted

[6]) W. Schottky, Small-shot effect and flicker effect, Phys. Rev. **28**, 74-103, 1926.

[7]) J. G. van Wijngaarden, K. M. van Vliet and C. J. van Leeuwen, Low-frequency noise in electron tubes, Physica **18**, 689-704, 1952.

[8]) See page 75 *et seq.* of the book by Van der Ziel mentioned in footnote [3]).

[9]) H. Groendijk, A noise diode for ultra-high frequencies, Philips tech. Rev. **20**, 108-110, 1958/59.

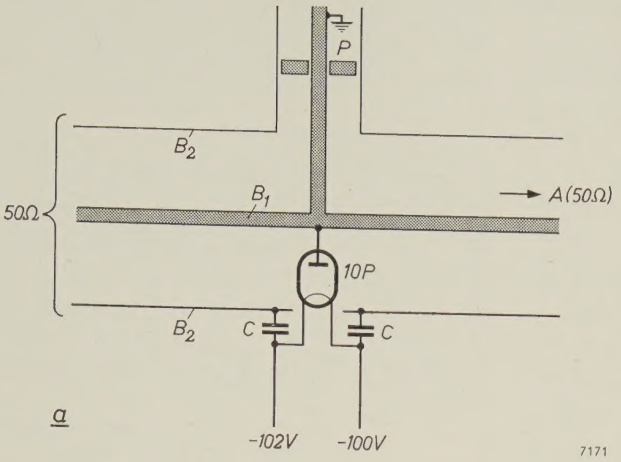

Fig. 8. Type 10 P noise diode in a coaxial system. *a*) Schematic cross-section, *b*) and *c*) side views. The diode projects through a hole in the outer conductor B_2, to which the filament is connected via the coupling capacitors C (each of capacitance $\frac{1}{2}C_1$). The anode is connected to the central conductor B_1. On the right in (*a*) is connected the four-terminal network under measurement; left, a matched termination. The shorting plunger P in the side tube is used to tune out the effects of the diode capacitance and the impedance of the coupling capacitors.

In a new valve holder (*b* and *c*) the capacitors C have a mica dielectric (shown black in the figure). The capacitor plates *1*, *3* and *5* are connected to the outer conductor B_2 of the coaxial system, plates *2* and *4* are connected to one side of the filament, plates *2'* and *4'* to the other side.

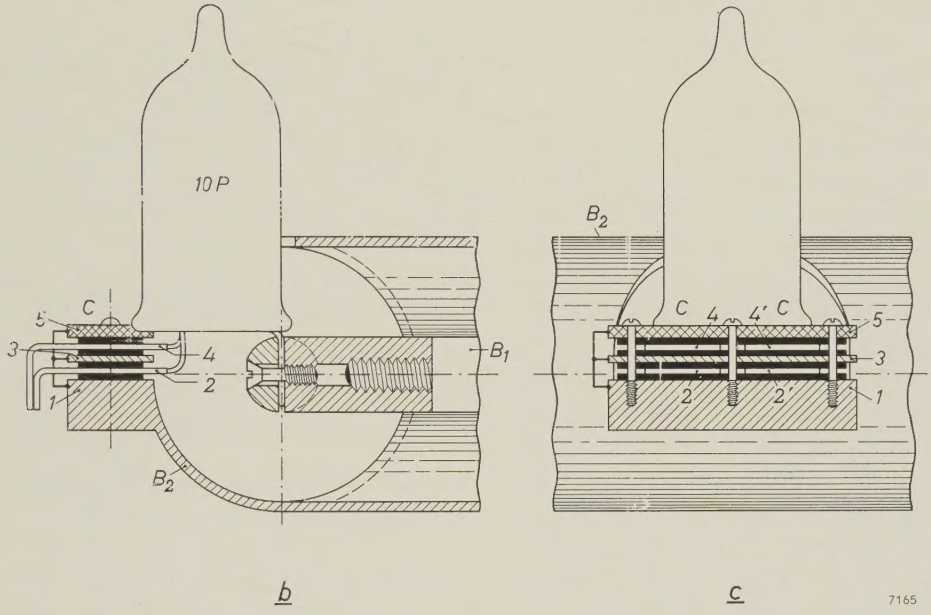

across the current source i' (fig. 9*b*); i' is the current which produces across the noiseless resistance R^* (fig. 9*c*) a noise voltage equal to the output noise voltage in fig. 9*a*. It can be calculated that the two circuits are equivalent at the frequency f if the following relation exists between the currents i' and i:

$$i' = \frac{i}{1 - (2\pi f)^2 L_0 C_0 + \mathrm{j} \times 2\pi f C_0 Z_1} \quad . \quad . \quad (10)$$

The impedance Z_1 of the two coupling capacitors in parallel can be reasonably approximated by the impedance of a capacitance C_1 and an inductance L_1 in series. Introducing a frequency f_t, defined by $(L_0 + L_1)C_0 = (2\pi f_t)^2$, we find from (10), after taking the mean square, the following expression for the *transformation factor* γ_t:

$$\gamma_t = \frac{\overline{i'^2}}{\overline{i^2}} = \left[1 - \left(\frac{f}{f_t}\right)^2 + \frac{C_0}{C_1}\right]^{-2} .$$

$1 - \gamma_t$ is the *transformation error* we wish to find.

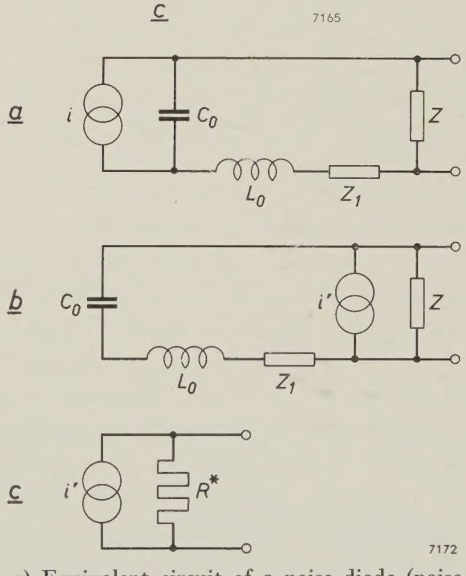

Fig. 9. *a*) Equivalent circuit of a noise diode (noise-current generator i), the capacitance of which is C_0; L_0 is the inductance of the lead-in wires, Z_1 the impedance of the coupling capacitors, and Z the impedance of the resistance R in parallel with a section of transmission line.

b) The current source i in (*a*) has been replaced by a current source i' in parallel with Z.

c) Equivalent circuit of (*b*), consisting of the current source i' in parallel with the noiseless resistance R^*.

There is no objection to raising the capacitance of the coupling capacitors sufficiently for C_1 to be large compared with the capacitance C_0 of the diode. In that case, at least at frequencies f not too close to f_t, we can disregard C_0/C_1, giving:

$$\gamma_t \approx \left[1 - \left(\frac{f}{f_t}\right)^2\right]^{-2} . \quad . \quad . \quad . \quad . \quad (11)$$

Fig. 10 shows a plot of γ_t versus f in accordance with (11), with f_t as parameter. At frequencies a great deal lower than f_t, the transformation factor γ_t is roughly 1, and the error therefore about zero. The value of f_t at which γ_t becomes 1.10 ($f = 0.22\ f_t$) is roughly the upper limit of the frequency range in which the diode can be regarded as an absolute noise standard; at higher frequencies the correction $1 - \gamma_t$ is too inaccurate.

From fig. 10 it can be seen that $1 - \gamma_t$ increases markedly with increasing f_t. The aim is therefore to make $f_t = 1/[2\pi\sqrt{(L_0 + L_1)C_0}]$ as high as possible and thus to minimize L_0, L_1 and C_0. Careful assembly of the diode and the proper choice of coupling capacitors are therefore of considerable importance in this respect. In the 10 P noise diode C_0 has the very low value of 1.8 pF. The values of L_0 and L_1 depend closely on the construction of the valve holder and the coupling capacitors. In the article cited [9]) a valve holder was described using ceramic coupling capacitors for coaxial systems. In a later model (fig. 8*b* and *c*) these capacitors were replaced by mica capacitors (of 230 pF each, so that $C_1 =$ 460 pF). From impedance measurements a value of 2900 Mc/s was found for the frequency f_t of the 10 P diode in this holder; noise measurements [10]) at 500 to 1500 Mc/s yielded values from 2600 to 3400 Mc/s, depending on the frequency. Comparison of these results with the resonance frequency of the diode itself: $1/(2\pi\sqrt{L_0C_0}) = 3500$ Mc/s, shows that the stray inductance L_1 is satisfactorily low.

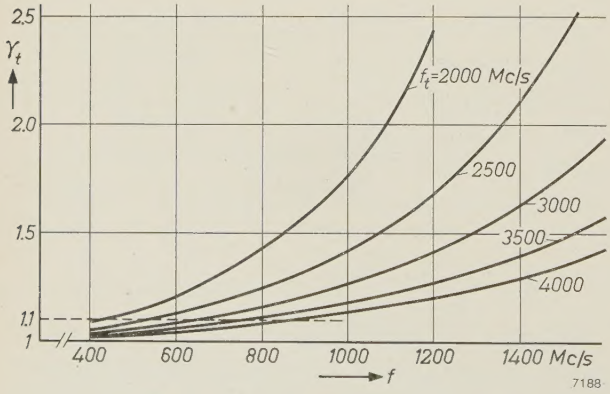

Fig. 10. The transformation factor γ_t, given by (11), as a function of frequency f, with the frequency f_t as parameter.

[10]) See p. 302 under "Experimental determination of $\gamma_t\gamma_\tau$".

The transit-time error

In a diode the electrons take a finite time to travel from the cathode to the anode. In diodes such as the 10 P type, of coaxial cylindrical construction with a cathode diameter of 0.1 mm and an anode diameter of 1 mm, and with an anode voltage V_a which is high enough for operation well within the saturation region, the electron transit time τ is:

$$\tau = \frac{1.08 \times 10^{-9}}{\sqrt{V_a}} \text{ second} \quad . \quad . \quad (12)$$

(with V_a in volts). During this time the electron induces a current pulse in the external circuit. Assuming that the current pulses of the different travelling electrons are mutually independent (i.e. that the electron emission is random and that there is no space charge), and moreover that the electrons leave the cathode radially and without an initial velocity, the noise current can be calculated by a suitable summation of the current pulses [11]). We then find that we must add to Schottky's formula (6) a transit-time factor γ_τ:

$$\overline{i^2} = 2\gamma_\tau q I_s \Delta f . \quad . \quad . \quad . \quad . \quad (13)$$

For the 10 P diode operating well within the saturation region this factor is given by:

$$\gamma_\tau = 1 - 2.67\ (f\tau)^2 ,$$

in which the terms in the fourth and higher powers of $f\tau$ are neglected. Using (12) we can then write:

$$\gamma_\tau = 1 - 3.13 \frac{f^2}{V_a} \times 10^{-18} . \quad . \quad (14)$$

It can be seen from (14) that at low frequencies γ_τ approaches unity, in which case (13) reduces to (6), the original Schottky equation. The use of (6) at higher frequencies gives rise to an error of $1 - \gamma_\tau$, the *transit-time error*.

It should be noted that the error is greater than follows from (14) if the anode voltage is so low that the diode is only barely saturated. One reason is that the assumption of radial emission without initial velocity is then no longer correct (an electron that does not leave the cathode radially is a longer time in transit than one that does, and consequently

[11]) E. Spenke, Die Frequenzabhängigkeit des Schroteffektes, Wiss. Veröff. Siemens-Werke **16**, No. 3, 127-136, 1937. G. Diemer and K. S. Knol, The noise of electronic valves at very high frequencies, I. The diode, Philips tech. Rev. **14**, 153-164, 1952/53.

induces a pulse of different shape). Another reason is that the space charge affects the potential gradient and so changes the transit time of the electrons. The result is that equations (12) and (14) are not valid if V_a is too low.

Some means is therefore needed of ascertaining whether the diode is saturated or not. This cannot be seen clearly enough from a plot of the diode current I_d ($\leqq I_s$) versus V_a. A sharper criterion can be derived from the variation with V_a of the factor Γ^2, which is a measure of the suppression of the space charge. This factor occurs in the formula for the shot noise of a diode at frequencies up to about 100 Mc/s:

$$\overline{i^2} = 2\Gamma^2 q I_d \Delta f .$$

The factor Γ^2, which is equal to unity at saturation, quickly drops to a low value if the diode becomes less saturated, making the space-charge effect perceptible. For a given value of V_a a maximum value of I_d can be indicated at which Γ^2 deviates from unity and saturation is thus no longer present.

Fig. 11 shows Γ^2 as a function of V_a, with I_d as

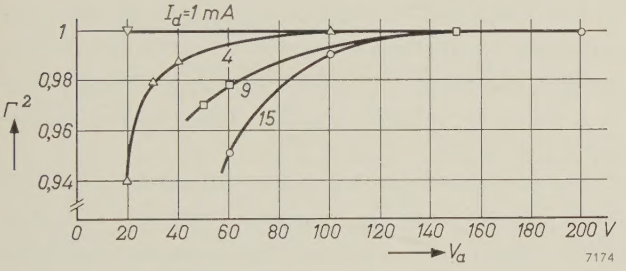

Fig. 11. The factor Γ^2 of the type 10 P noise diode at 30 Mc/s as a function of anode voltage V_a, for various values of the diode current I_d.

parameter, for the 10 P diode at 30 Mc/s. From this we can determine what the minimum V_a must be, at given values of I_d, if Γ^2 is not to differ by more than 1%, 2% or 3% from unity; see *fig. 12*. The values of V_a at which the anode dissipation $I_d V_a$ reaches 2 W, which is the maximum permissible value for the 10 P diode, are also shown in this figure; operation in the shaded region is thus not permissible.

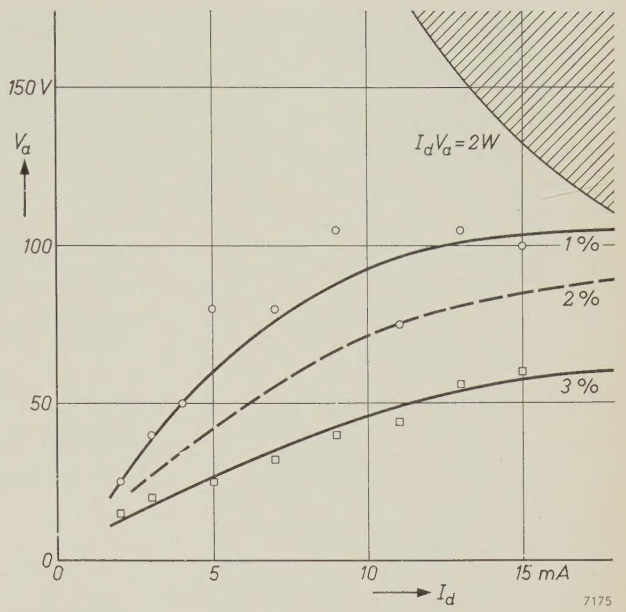

Fig. 12. Anode voltage V_a of type 10 P noise diode as a function of diode current I_d, with Γ^2 differing from unity by 1%, 2% and 3%, respectively. Curve $I_d V_a$ = 2 W indicates the values of V_a at which $I_d V_a$ = 2 W.

Transformation and transit-time errors combined

In general, both errors are present and must be taken into account:

$$\overline{i'^2} = 2\gamma_t \gamma_\tau q I_s \Delta f .$$

The highest frequency, then, at which the Schottky formula is still applicable is that where $\gamma_t \gamma_\tau$ only just permissibly deviates from unity. Having regard to the accuracy required for most noise measurements, the deviation is usually fixed at 10%. If $\gamma_t \gamma_\tau$ is known in a particular frequency range, the Schottky formula can be corrected to enable the diode to be used in that range.

From (11) and (14) it appears that, where f is smaller than f_t, the two γ factors differ from 1 in opposite senses: γ_t is greater than 1 and γ_τ is smaller. The two errors, then, compensate one another to some extent. In usual conditions γ_t differs more from 1 than γ_τ. The compensation can therefore be improved, i.e. the product $\gamma_t \gamma_\tau$ brought closer to unity, by increasing the electron transit time. This can be done by lowering the anode voltage (*fig. 13a*), but not so far that the diode ceases to be saturated; otherwise a space charge would form and γ_τ would then depend on the diode current. The space-charge effect may be greater at high frequencies (of the order of 1 Gc/s) than at lower.

The magnitude of the effect of lowering the anode voltage can only be roughly estimated, because the diode then enters a region where (14) is no longer valid. Calibration is therefore necessary. We can see this plainly by comparing fig. 13*a* with fig. 13*b*. Both graphs give γ_τ as a function of frequency for various values of the anode voltage; fig. 13*a* gives values calculated from (14), and fig. 13*b* measured values. It is assumed that γ_τ for V_a = 300 V varies in accordance with (14); theory and measurements indicate that this will be correct to within about 2%.

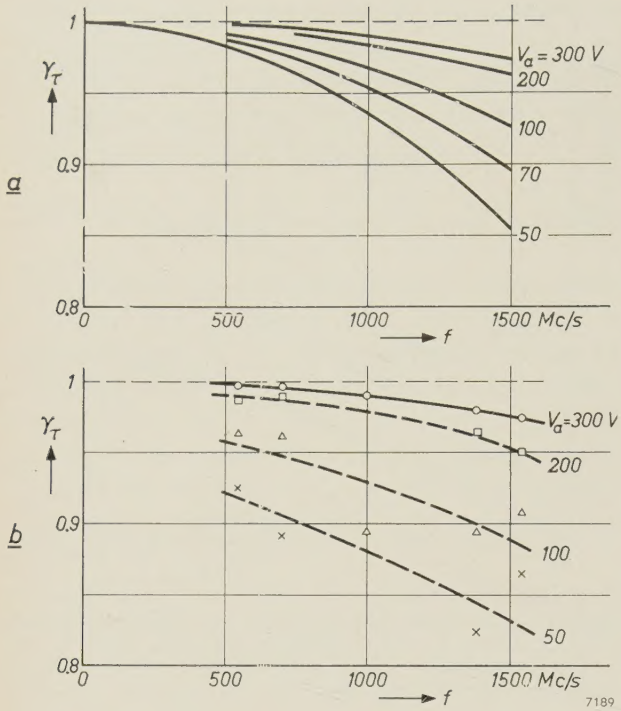

Fig. 13. *a*) *Calculated* values of the transit-time factor γ_τ of a 10 P noise diode as a function of frequency f, with the anode voltage V_a as parameter.
b) *Measured* values of γ_τ for V_a = 200, 100 and 50 V, in relation to the calculated values for V_a = 300 V.

The values of γ_τ measured at V_a = 200, 100 and 50 V are plotted in relation to the calculated values for V_a = 300 V. (As will appear in the next section, γ_τ by itself cannot be measured but the product $\gamma_t\gamma_\tau$ can.) We see from fig. 13*a* and *b* that the measured γ_τ differs increasingly from the calculated values as the anode voltage is reduced: the average discrepancy is about 1% at V_a = 200 V, about 4% at 100 V, and about 5% at 50 V.

In *fig. 14* the calculated and measured values of $\gamma_t\gamma_\tau$ for the 10 P diode are plotted versus frequency,

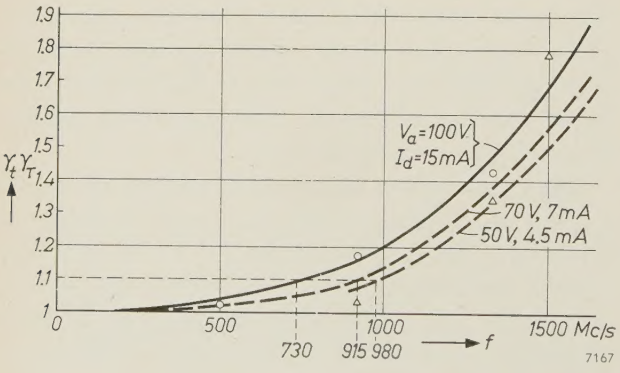

Fig. 14. The curves give the calculated values of $\gamma_t\gamma_\tau$ for a 10 P noise diode with various combinations of V_a and I_d. The experimental points indicated all relate to V_a = 100 V; the circles relate to comparison with a cold standard noise source, the triangles to comparison with a gas-discharge noise source as in fig. 17*a*, which was previously calibrated with a hot standard noise source.

with V_a as parameter. Lowering V_a from 100 to 50 V widens the frequency range from about 730 to about 980 Mc/s, a gain of 35%. Set against this is the great disadvantage that the diode current at V_a = 50 V should not be more than 4.5 mA, as otherwise the factor I'^2 will deviate by more than 1% from unity; see fig. 12. At such a low diode current only small noise factors can be measured satisfactorily, large ones not, at least not without correction.

Experimental determination of $\gamma_t\gamma_\tau$

The quantity $\gamma_t\gamma_\tau$ has been determined experimentally [12]) in the following way. A resistor $R(T_1)$ is held at room temperature, and a resistor $R(T_2)$ of roughly the same value at 77 °K (in liquid nitrogen). Both are provided with a variable impedance transformer (e.g. of the type sketched in fig. 3), which has the same temperature as the appertaining resistor. First of all, the transformed resistance of one of the resistors is made as nearly as possible equal (to within about 5%) to 50 ohm, by means of a standing-wave detector. This resistor is then connected via a coaxial switch to a bridge circuit (which need not be calibrated), after which the bridge is balanced. The second resistor is connected to the bridge by turning the switch, and the relevant impedance transformer is adjusted until the bridge is again balanced. This substitutional method makes it possible to equalize the two resistances with an accuracy up to 0.1%.

The next step is to assemble the circuit indicated in *fig. 15*: behind the switch S come a 10 P noise diode in a coaxial holder [13]), a superheterodyne

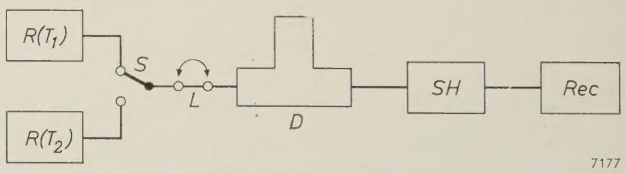

Fig. 15. Measurement of $\gamma_t\gamma_\tau$. The resistors $R(T_1)$ and $R(T_2)$ have as nearly as possible the same value R ($\approx$ 50 ohm) at the respective temperatures T_1 ($\approx$ room temperature) and T_2 (= 77 °K). *D* noise diode type 10 P in coaxial holder. *SH* superheterodyne receiver. *Rec* recorder. When switch *S* is in the position as drawn and the diode is without filament current, the recorder gives a certain deflection. When *S* is in the other position, the filament current is adjusted so as to produce the same deflection on the recorder. Using eq. (15) it is then possible to calculate $\gamma_t\gamma_\tau$.

At *L* a coaxial line of 50 ohm characteristic impedance and a quarter wavelength long can be inserted for a second measurement, to reduce the error caused by the fact that $R(T_1)$ and $R(T_2)$ do not have exactly the same values.

[12]) By W. E. C. Dijkstra of this laboratory.
[13]) The switch with resistors thus takes the place of the anode resistor of 50 ohm described in the article mentioned in footnote [9]).

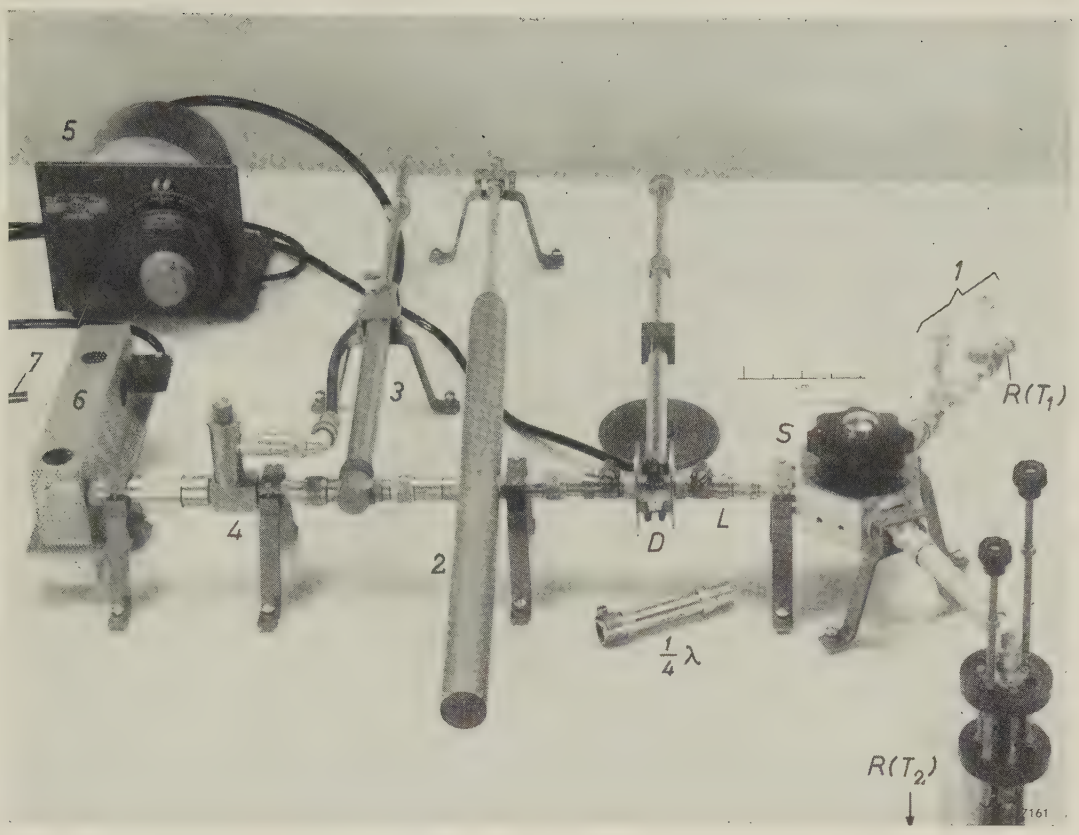

Fig. 16. Part of the equipment for measuring $\gamma_t\gamma_\tau$ at decimetre wavelengths by the method illustrated in fig. 15. $R(T_1)$ standard noise resistor at room temperature, with matching transformer *1*. $R(T_2)$ standard noise resistor at 77 °K as in figs 3 and 4 (only the upper part of the impedance transformer can be seen). *S* coaxial switch. *D* noise diode type 10 P in holder as shown in fig. 8. At *L* a section of waveguide a quarter wave in length can be inserted.

The equipment to the left of *D* is part of the superhet receiver: *2* coaxial resonant cavity, functioning as a filter that only passes a narrow band of frequencies around the measuring frequency *f* (it therefore does not pass the frequency of the local oscillator, nor the image frequency); *3* impedance transformer for matching the crystal mixer *4* to the resonant cavity *2*; *5* local oscillator; *6* first and second stages of the IF amplifier (30 Mc/s); *7* cable to the remaining part of the IF amplifier.

receiver and a recorder. Some of the equipment can be seen in *fig. 16*.

The resistor $R(T_1)$ is now switched in, the diode not yet passing any filament current. The noise of $R(T_1)$, which reaches the receiver through the switch and the diode holder, produces a certain deflection on the recorder. After switching over to $R(T_2)$ the filament current of the diode is adjusted until the recorder shows the same deflection as before. The noise produced by the resistor at 77 °K together with the diode is then equal to the noise of the resistor alone at the temperature T_1. For this condition we easily arrive at the following formula for $\gamma_t\gamma_\tau$:

$$\gamma_t\gamma_\tau = \frac{T_1 - 77}{RT_0 I_s \times 20}. \quad \ldots \quad (15)$$

An important point is that the receiver requires no calibration. Since R occurs in the formula, however, its value must be accurately known.

The effect of a small error ΔR in R can be reduced by a simple expedient: *two* measurements are done as described above, but in the second we insert between the switch and the diode holder, at *L* in fig. 15, a coaxial line whose characteristic impedance is 50 ohm and which is a quarter wavelength long. In (15) we must then replace R by

$$R' = \frac{50^2}{50 + \Delta R} \approx 50 - \Delta R.$$

The error in R', then, is just as great as in R, but of opposite sign; the average of $\gamma_t\gamma_\tau$ from the two measurements is therefore more accurate than the result of one measurement. A condition, however, is that the characteristic impedance of the inserted line must be more exactly equal to 50 ohms than R, otherwise the improvement is illusory.

Summarizing, it can be said that the 10 P diode, with $V_a = 100$ V and $I_d = 15$ mA, can be used without correction as a standard noise source from about 100 c/s to about 730 Mc/s, the maximum error being 10%. At higher frequencies either correction or compensation is necessary. With wide-

band circuits, compensation has the advantage that the noise does not depend on the frequency.

It should also be noted that in certain applications, where for instance the equipment has to be adjusted for minimum noise, only relative noise differences are important; what is needed here, then, is a constant source, which need not be a standard one. For example, the automatic noise-figure indicator mentioned [1]) in combination with a 10 P diode has proved very useful for adjusting 4 Gc/s equipment for minimum noise, and this is certainly not the highest frequency at which this is possible.

The gas discharge as a noise source

Mechanism of noise generation by a gas discharge

The positive column of a gas discharge emits electromagnetic radiation having the character of noise. In the centimetre and millimetre wavebands the column of an inert-gas discharge, which is both long and strongly coupled to the measuring circuit, is a particularly suitable noise source for the purposes of measurement.

The positive column consists of ions, electrons and neutral particles. There are roughly just as many positive elementary charges per unit volume as there are negative ones. Such a quasi-neutral mixture is called a *plasma*. The electrons in the plasma have a much higher average velocity than the ions and the neutral particles. This is due to their very low mass (compared with the other particles) as a result of which they are much more accelerated in the electric field and moreover lose very little energy upon elastic collisions with heavy particles.

Owing to the deceleration which an electron suffers upon a collision, a small fraction of its energy is converted into electromagnetic radiation ("Bremsstrahlung"). Since the velocities of the electrons show a random distribution, both in magnitude and direction, the emitted radiation has the character of noise. The power of this radiation depends on the average kinetic energy of the electrons upon collision, that is on the "electron temperature" T_{el}. Let the mass of an electron be m and the mean square velocity be $\overline{v^2}$, then T_{el} is defined as:

$$\tfrac{1}{2}m\,\overline{v^2} = \tfrac{3}{2}\,k\,T_{el}\,.$$

Because the average energy of an electron is much greater than that of the other particles, T_{el} is a high temperature (of the order of 10^4 °K), much higher than the temperature of the gas, which as a rule is not much above room temperature.

It may be asked how the power radiated by the plasma depends on T_{el}. If either the electron velocities show a Maxwell distribution, or the collision frequency is constant, the radiant power of the plasma is equal to the noise power available from a resistor at the temperature T_{el} [14]), in other words in a small frequency band Δf it is equal to $kT_{el}\,\Delta f$. Experiments have shown [15]) that even though the above conditions are not entirely fulfilled, $kT_{el}\,\Delta f$ can be a good approximation for the power radiated by a plasma in the band Δf. In most cases, then, the power can be assumed to have this value.

Various forms of gas-discharge noise sources

A simple form of gas-discharge noise source consists of a gas-discharge tube mounted in a resonant cavity, with an impedance-matching transformer. This construction is useful for physical research on plasmas, but does not constitute a noise source suitable for a wide range of frequencies. Such a source can be realized, however, in another way. Three examples are given in *fig. 17*; the frequency ranges for which they are suitable will be found in fig. 1 (lines *I* and *II*).

The constructions in fig. 17, although differing considerably from one another, are all based on the same principle. We can make this clear with the aid of the diagram in *fig. 18*. This figure represents the longitudinal cross-section of a waveguide, which has a matched termination at one end in the form of an absorption wedge A, whose temperature is T_1. From B to C extends a homogeneous plasma which, we shall assume, fills the entire cross-section of the waveguide.

Both the wedge A and the plasma emit noise waves. The *wedge* sends out noise waves (power P_A, temperature T_1) from A to D. The waves, after passing through the plasma, where they are attenuated, have the lower power P_A' corresponding to a temperature lower than T_1. The *plasma* sends out noise waves to left and right, having powers P_B and P_C, which can be calculated by integrating the emission over the whole plasma column. The wave P_B is completely absorbed in the wedge A, and may therefore be left out of further consideration. The wave leaving the noise generator at D has an equivalent noise temperature T_{eq}, which is the sum of the temperatures corresponding to P_A' and P_C (this summation is permissible owing to the fact that

---

[14]) G. Bekefi and S. C. Brown, Microwave measurements of the radiation temperature of plasmas, J. appl. Phys. **32**, 25-30, 1961 (No. 1).
G. H. Plantinga, The noise temperature of a plasma, Philips Res. Repts **16**, 462-468, 1961 (No. 5).

[15]) K. S. Knol, Determination of the electron temperature in gas discharges by noise measurements, Philips Res. Repts **6**, 288-302, 1951.

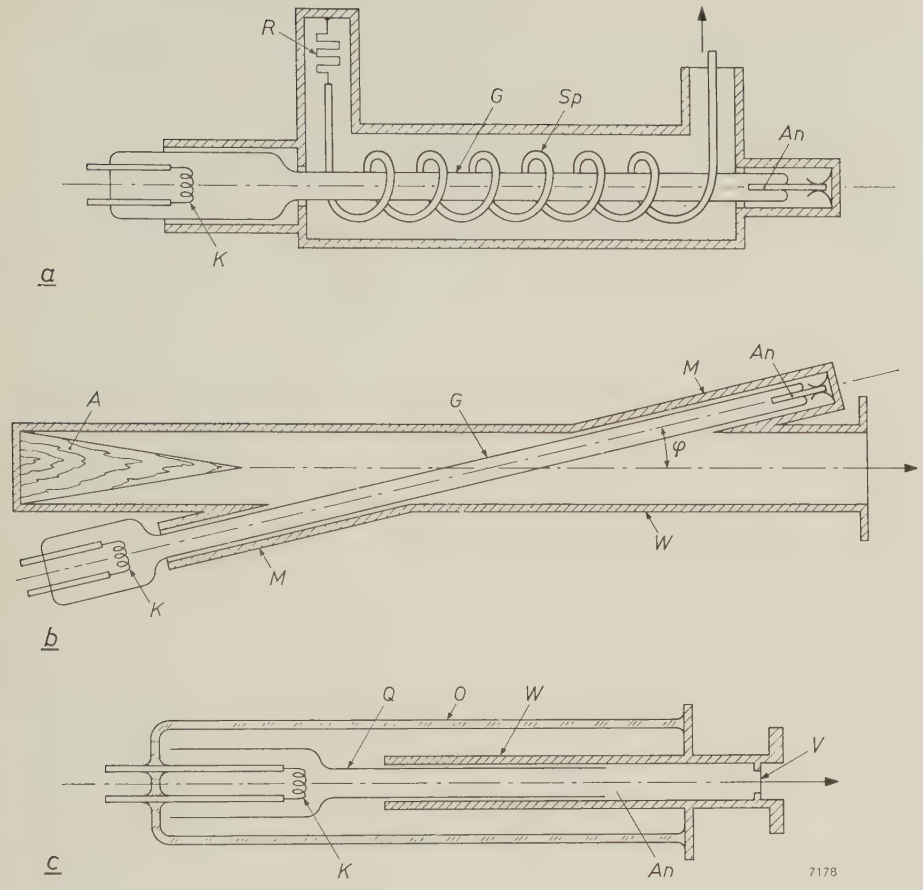

Fig. 17. Three constructions of gas-discharge noise sources. *G* gas discharge tube with cathode *K* and anode *An*.

a) Construction for decimetre waves. The discharge tube is coupled via the helix *Sp* to a system which has a matched termination on the left in the form of a resistor *R*, and on the right goes over into a coaxial system.

b) Construction for centimetre waves, the discharge tube passing obliquely through the waveguide *W* with side arms *M*. *A* is an absorption wedge providing a matched termination.

c) Construction with axial gas discharge in a circular waveguide *W*, for millimetre waves. *Q* thin-walled tube of quartz glass, open at both ends. The glass envelope *O* is filled with neon. *V* mica window. The inside wall of the waveguide *W* just past one end of the tube *Q* serves as anode (*An*).

the two noise waves are mutually independent). Thus,

$$T_{eq} = T_A' + T_C\,.$$

If L is the attenuation suffered by the power of the waves in passing through the entire plasma column, we can write

$$T_{eq} = \frac{1}{L}\,T_1 + \left(1 - \frac{1}{L}\right) T_{el}\,. \qquad (16)$$

It is assumed here that the reflections at the boundary planes B and C are negligible. (Reflection from C lowers the equivalent temperature T_{eq}; reflection from B lowers or raises T_{eq}, depending on whether the waves are in phase or in anti-phase.) If L is sufficiently large, T_{eq} differs very little from T_{el}, and reflections from B have no further perceptible influence, no more than has the temperature T_1.

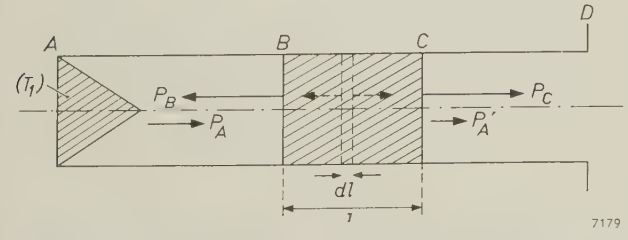

Fig. 18. Illustrating the principle shared by the three designs in fig. 17. *AD* waveguide terminated at the left by an absorption wedge, with a plasma between *B* and *C*. The plasma sends out noise waves to left and right, having a power P_B and P_C respectively; the wedge emits noise waves with a power P_A, which are attenuated in the plasma to the power P_A'.

Equation (16) can be derived as follows. We imagine that the wedge A is heated to a temperature equal to T_{el}. According to the Nyquist theorem, the total noise power in the band Δf which goes to D must be equal to $kT_{el}\,\Delta f$, for to the left of C everything is at the temperature T_{el} (the plasma being equivalent to an absorption medium at the temperature T_{el}), and we have assumed that there are no reflections. To the power passing from C to D the wedge A contributes $L^{-1}\,kT_{el}\,\Delta f$. The plasma contribution is therefore $(1 - L^{-1})kT_{el}\Delta f$. When the wedge is now cooled to the temperature T_1, its contribution drops to $L^{-1}kT_1\Delta f$, whereas that of the plasma shows no change. The total is thus:

$$kT_{eq}\Delta f = L^{-1}\,kT_1\Delta f + (1 - L^{-1})kT_{el}\Delta f\,,$$

which leads directly to eq. (16).

Some requirements which must be met by a gas-discharge noise source

In order to build a gas-discharge noise source that will deliver a high and constant noise power in a broad range of frequencies, it is necessary, as we have seen, to start with a plasma of high electron temperature T_{el}, and to introduce this in the circuit

in such a way that the attenuation L is high and there are no reflections at the boundary plane C (fig. 18).

The electron temperature depends in a complicated manner on the kind of gas used, the gas pressure, the temperature of the column and the discharge current. In inert-gas discharges, T_{el} increases with a decrease in the atomic weight of the gas or its pressure, or the column diameter or the current density [15][16]). Under otherwise identical conditions, therefore, helium gives the highest electron temperature. For various reasons, however — including the short life obtained with helium and the considerable heat generated in a helium discharge — the lightest but one inert gas is preferred, namely neon.

The requirement of a high attenuation L was difficult to fulfil in the millimetre wavebands, and necessitated a new design. The elimination of reflections at C gave the greatest difficulties in the decimetre range. To provide some insight into these problems, we shall consider the complex relative dielectric constant ε_r that can be assigned to a plasma. The imaginary part of ε_r relates to the dissipation, and the ratio of the imaginary to the real part relates to the phase shift:

$$\varepsilon_r = 1 - \frac{\omega_p^2}{\omega^2 + \nu^2} + j\frac{\omega_p^2 \nu}{\omega(\omega^2 + \nu^2)} . \quad . (17)$$

Here ω_p is the plasma frequency, given by $\omega_p = qN^2/\varepsilon_0 m$ (where N is the electron density and ε_0 the dielectric constant of free space), ω is the angular frequency of the wave, and ν the average collision frequency; we assume that ν does not depend on the electron velocity. It may be concluded from (17) that for any given plasma (given ω_p and ν) ε_r is closer to unity the higher is the angular frequency ω, i.e. the shorter the wave. If the remainder of the waveguide in fig. 18 is filled with a non-ionized gas (e.g. air) for which $\varepsilon_r = 1$, there will be no reflection at the boundary planes. However, the absorption in the gas — and hence the attenuation L — shows a marked decrease, for as ω increases, the imaginary part of ε_r approaches zero. A high attenuation L can therefore only be obtained by filling the waveguide with plasma *over a considerable length.*

The construction that most closely approaches this schematic picture is that shown in fig. 17*c*. Before discussing this, we shall consider the more conventional designs sketched in fig. 17*a* and *b*.

A gas-discharge noise source for decimetre waves

Since waveguides for decimetre waves would have to be very large, *coaxial* systems are generally used in this wave range. A suitable noise source can be seen in fig. 17*a*. A gas-discharge tube G, e.g. a type K 50 A tube, is placed inside a silver-plated helix Sp, which effects the coupling with the gas discharge and at each end passes into the central conductor of a coaxial system. The coupling takes place over the entire length of the helix, and thus has the gradual nature that enables the reflection to be kept at a very low value. One end of the helix is connected to a matched termination (the resistance R of temperature T_1). The helix is dimensioned so that it has a characteristic impedance of 50 ohm, equal to that of the output plug.

Further particulars of the dimensioning will be found in the literature [17]).

A gas-discharge noise source for centimetre waves

Fig. 17*b* shows the commonly used system designed by Johnson and Deremer for waveguides of not all too small dimensions [18]). The gradual transition between the column and the waveguide — necessary for minimizing reflections from the column — is obtained here by passing the gas-discharge tube obliquely through the waveguide (at an angle φ). The tube current (on which ω_p depends, see eq. 17) and the angle φ can be chosen in such a way that the reflection from the column is practically zero. At one end the waveguide has a matched termination in the form of an absorption wedge.

Since the cathode and anode of the tube are outside the waveguide, there is a danger that a considerable part of the noise power will be lost through the side arms M which contain the discharge tube. To avoid such losses, the arms are made so narrow that their lowest cut-off frequency is higher than the operating frequency of the noise generator. This means, of course, that the cross-section of the column must be quite a bit smaller than that of the waveguide; as a result the attenuation L is not maximum, but this is not a serious objection in the centimetre waveband, where the attenuation is still amply sufficient for the purposes for which it is used.

Table I gives some equivalent noise temperatures obtained in our laboratory with noise generators of

[16]) A. von Engel and M. Steenbeck, Elektrische Gasentladungen, Part II, Springer, Berlin 1934, p. 85 *et seq.*
F. M. Penning, Electrical discharges in gases, Philips Technical Library 1957, p. 58 *et seq.*

[17]) H. Schnittger and D. Weber, Über einen Gasentladungs-Rauschgenerator mit Verzögerungsleitung, Nachr.-techn. Fachber. **2**, 118-120, 1955.

[18]) H. Johnson and K. R. Deremer, Gaseous discharge super-high-frequency noise sources, Proc. Inst. Radio Engrs **39**, 908-914, 1951.

Table I. Equivalent noise temperatures obtained with various types of discharge tube in the noise generator shown in fig. 17*b* (except for the last line, which relates to the construction in fig. 17*c*).

Freq.	Wavelength	Gas-discharge tubes				Equivalent noise temperature
		type	gas	pressure	current	
Gc/s	cm			torr	mA	°K
4	7.5	K 51 A	Ne		200	23 800
		exper.	Xe	10	150	9 550
6	5	exper.	Ne	8	125	23 400
		exper.	Ar	8	125	14 000
10	3	exper.	He	10	125	28 000
		K 50 A	Ne		125	21 700
		exper.	Ar	8	125	14 000
		exper.	Xe	5.5	125	9 400
34	0.88	exper.	He	40	100	22 700
		exper.	Ne	90	100	20 600
		exper.	Ar	40	75	13 400
		exper.	Kr	20	95	11 200
		exper.	Xe	8	75	9 200
75	0.40	exper.	Ne	100	75	21 000

this type [19]); a few of the discharge tubes employed are shown in *fig. 19*. It can be seen from the table that high noise temperatures T_{eq} are achieved with helium, in accordance with the expected high electron temperature T_{el}. We have already mentioned, however, some of the reasons why this gas is nevertheless unsuitable (short life, excessive heat generation). A further reason is that, with helium, T_{el} (and hence T_{eq}) is highly dependent on impurities in the gas. Neon does not have these drawbacks and the noise temperatures obtained are only in a few cases lower than those achieved with helium; this is attributable to the high attenuation L which is possible in neon [19]). Neon is therefore the gas preferred in practice.

It is also important to note that the values of T_{eq} obtained with neon are fairly close to one another, in spite of the markedly divergent conditions (gas pressure, current and frequency), which promises well for its usefulness at even higher frequencies.

[19]) For further details of experiments at frequencies from 10 to 75 Gc/s see: P. A. H. Hart and G. H. Plantinga, Millimetrewave noise of a plasma, Proc. 5th Internat. Conf. on ionization phenomena in gases, Munich 1961, pp. 492-499 (North-Holland Publishing Co., Amsterdam 1962).

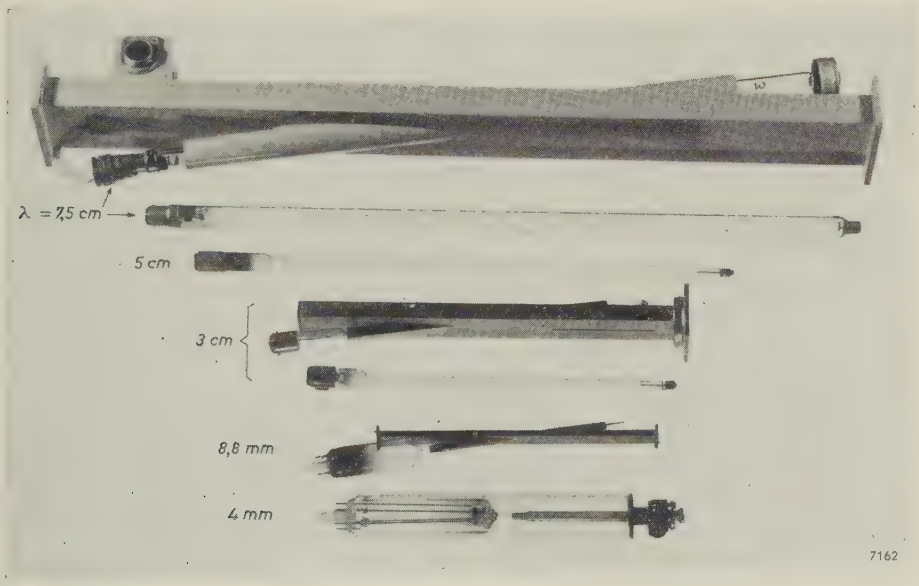

Fig. 19. Experimental gas-discharge noise sources. From top to bottom:
a 7.5 cm waveguide with discharge tube passing obliquely through it,
the 7.5 cm tube separately,
a tube for 5 cm wavelength,
a 3 cm waveguide with tube,
the 3 cm tube separately,
an 8.8 mm waveguide with tube,
a 4 mm tube as described in reference [20]).
The tubes are all shown with the cathode on the left and the anode on the right, the waveguides with the output on the right.

A gas-discharge noise source for millimetre waves

The small dimensions of waveguides for waves shorter than about 8 mm make the construction in fig. 17*b* difficult for practical reasons. For millimetre waves the construction shown in fig. 17*c* is more suitable; this was described some time ago in this review [20]), and can therefore be dealt with here very briefly.

In a circular waveguide W (fig. 17*c*) a thin-walled tube Q of quartz glass is introduced. A flared part of the tube contains the oxide cathode K for the gas discharge. The neon is contained (at a pressure of 100 torr) in the tube Q, and also in the waveguide, which is closed at V by a mica window. Since the mean free path in the gas is very short (approx. 6.5 μ), the plasma ends fairly abruptly where the quartz-glass tube ends, and at that position, at An, the anode is formed by the inside of the waveguide; beyond that point, then, the neon is not ionized. The last line of Table I relates to a tube of this type.

From equation (16) we saw that a high attenua-

[20]) P. A. H. Hart and G. H. Plantinga, An experimental noise generator for millimetre waves, Philips tech. Rev. **22**, 391-392, 1960/61 (No. 12).

tion L is necessary for matching in a wide range of frequencies. In this construction, the attenuation is obtained through the column, which is here in the axial direction of the waveguide. Since a column can be made arbitrarily long (provided the applied voltage is high enough), the attenuation can in principle be made as large as required by simply making the quartz-glass tube and the waveguide long enough.

The wall of the quartz-glass tube is made very thin (about 0.1 mm); this gives the filling factor of the plasma in the waveguide a high value and limits the losses resulting from noise power leaking away along the tube.

As indicated in the last line of Table I, a noise temperature of 21 000 °K has been achieved at a wavelength of 4 mm.

We shall now briefly consider what the minimum and maximum frequencies are for the noise generator of fig. 17*c*.

Minimum frequency

The lower the frequency, the larger must be the diameter of the waveguide. This has adverse consequences for the gas discharge. The diameter of a positive column cannot be widened indefinitely without giving rise to effects such as constriction and striations. The positive column then gradually loses its character and the electron temperature drops. Moreover, as seen from equation (17), as ω decreases the relative dielectric constant differs more and more from unity; this makes it evident that the abrupt ending of the column at the anode will increasingly give rise to reflection.

For these reasons the lowest frequency at which the noise generator in fig. 17*c* can be used with advantage is in the region of 35 Gc/s.

Maximum frequency

With increasing frequency the attenuation of the column per unit length decreases. To keep L large enough, it is therefore necessary to make the column and the waveguide longer. Lengthening the waveguide increases the losses in the waveguide wall. There is thus a danger that these losses will finally predominate. The noise would then largely be due to the guide wall, whose temperature is relatively low (400 to 500 °K).

One way of getting around this difficulty is to make the waveguide relatively wide. For a wavelength of 4 mm, for example, we have made the inside diameter of the waveguide 4 mm. Outside the noise generator a gradual transition is then needed to the usual rectangular waveguide.

The upper limiting frequency is probably higher than 300 Gc/s.

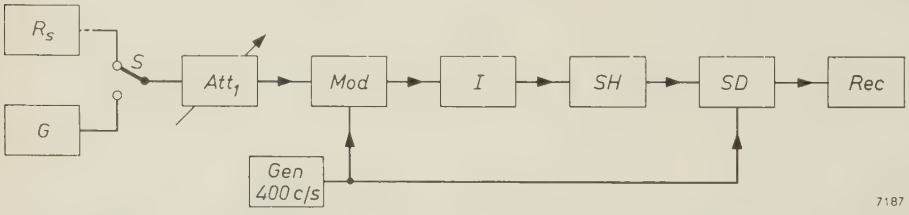

Fig. 20. Calibration of a gas-discharge tube G with a standard noise resistor R_s. S switch. Att_1 calibrated attenuator. *Mod* modulator (directional isolator) which modulates the noise with a 400 c/s signal delivered by the generator *Gen*. *SH* superhet receiver. *SD* synchronous detector. *Rec* recorder. *I* directional isolator which prevents the noise from *SH* from reaching the modulator (this noise would otherwise be modulated and cause errors).

Calibration of gas-discharge noise sources

A resistor, and also a noise diode (at least in a wide range of frequencies) can be regarded as absolute noise standards; a gas discharge, however, cannot be so regarded and must therefore be calibrated. To conclude this article, we shall briefly consider this process of calibration.

Our gas-discharge noise sources were calibrated by comparing them with a standard noise source. This consisted of a resistance in the form of an absorption wedge (the matched termination in fig. 17) whose temperature was adjusted as accurately as possible to 1336 °K, the melting point of gold [5]).

Fig. 20 shows a simplified block diagram of the set-up; the major part of the equipment can be seen in *fig. 21*. The part on the right of the switch is a somewhat simplified version of Dicke's noise receiver, as used in radio astronomy [21]). This consists essentially of a modulator *Mod*, which modulates the incoming noise with an audio signal (400 c/s), followed by a superheterodyne system *SH*, a synchronous detector *SD* and a recorder *Rec*. In the synchronous detector the output signal from the superhet receiver is compared with the 400 c/s signal, with the result that the recorder responds only to a signal modulated with 400 c/s, i.e. to the incoming noise.

The modulator is a modified version of a directional isolator using Faraday rotation [22]). The modi-

[21]) R. H. Dicke, The measurement of thermal radiation at microwave frequencies, Rev. sci. Instr. **17**, 268-275, 1946. See also: C. A. Muller, A receiver for the radio waves from interstellar hydrogen, II. Design of the receiver, Philips tech. Rev. **17**, 351-361, 1955/56.

[22]) H. G. Beljers, The application of ferroxcube in unidirectional waveguides and its bearing on the principle of reciprocity, Philips tech. Rev. **18**, 158-166, 1956/57.

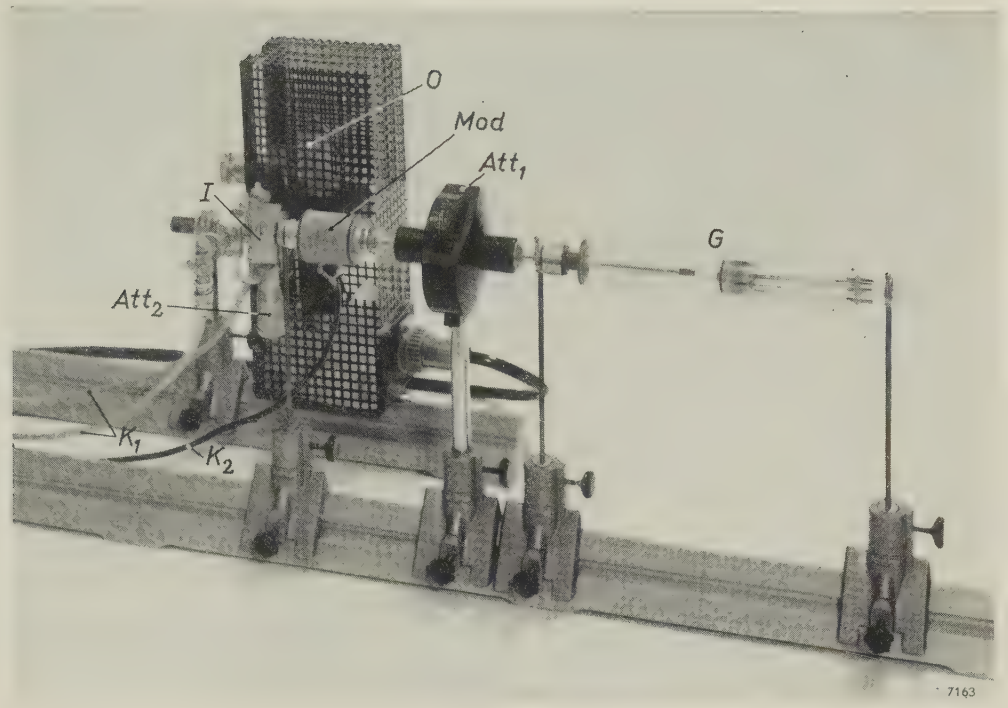

Fig. 21. Part of the equipment for calibrating the gas-discharge tube *G* (here a 4 mm tube). For Att_1, *Mod* and *I*, see fig. 20. *O* local oscillator (4 mm klystron) of the superhet receiver. Att_2 variable attenuator for adjusting the signal from *O* to the correct value. The cables K_1 go to the IF amplifier (with push-pull input); cable K_2 comes from the 400 c/s oscillator.

fication consists in the permanent magnet having been replaced by an electromagnet, which is energized by the 400 c/s signal. To prevent the inherent noise of the receiver also being modulated via reflections from the modulator, a second directional isolator is inserted between the modulator and the superhet receiver.

The procedure of calibration is as follows. First of all, the modulator is connected to the standard noise source R_s via a variable attenuator Att_1 set at minimum attenuation; the recorder shows a certain deflection. Next, the attenuator is connected to the gas-discharge noise source *G*, and the attenuation is adjusted until the recorder shows the same deflection as before. The gas-discharge noise source together with the attenuator now delivers just as much noise as the standard source.

Now the equivalent temperature T_{eq} of the gas-discharge noise source is given by

$$T_{eq} = B\,T_s' - (B-1)\,T_1\,,$$

where B is the inserted attenuation (including the attenuation due to losses in the line), T_1 the temperature of the attenuator, and T_s' the temperature (corrected for line losses) of the standard noise source.

As mentioned at the beginning of this article, gas-discharge noise sources are relatively insensitive to fluctuations in supply voltages and in ambient temperature, so that after calibration they can serve as sub-standards. Because of their reproducibility, it is not necessary to calibrate them individually; it is sufficient to calibrate a few samples.

Summary. Survey of the three main types of standard noise source: resistors, saturated diodes and gas discharges.

Resistors can be used as noise standards at frequencies ranging from the lowest to the ultra-high, in the order of 100 Gc/s (mm waves). For measuring the noise factor of a four-terminal network, two noise resistors are needed, one of which has the same resistance at the temperature T_1 as the other at the temperature T_2. Usually T_1 is made roughly equal to room temperature, and T_2 much higher or much lower. Examples discussed are a cold resistor for a coaxial decimetre-wave system ($T_2 = 77$ °K, bath of liquid nitrogen) and a hot resistor, mounted in a waveguide, for centimetre or millimetre waves ($T_2 = 1336$ °K, in an oven).

Dealing with the *saturated diode*, the author examines the limits of the useful frequency range. The lower limit is set by flicker noise and lies between 10 and 1000 c/s. The upper limit depends on the extent to which two errors occur: the transformation error and the transit-time error. The correction and mutual compensation of these errors are discussed. The type 10 P noise diode can be used in a new type of holder, without correction, up to 730 Mc/s.

On the subject of *gas-discharge* noise sources, the mechanism of the noise generation is examined. Three noise generators of this kind are reviewed: one for the decimetre band, one for the centimetre band and one for the millimetre band; they differ in the method of coupling the plasma with the waveguide. The article ends with a description of the calibration of this type of noise source.

A PHOTORECTIFYING LAYER FOR A READING MATRIX

by J. G. van SANTEN *) and G. DIEMER *).

621.383.44:621.319.2

Photoconductive materials have already proved their usefulness in many fields; we may mention the use of photocells for flame monitoring in oil-heating systems and for crackle-free volume control in radio receivers, and the use of photocathodes for pick-up tubes in television cameras. The use of photoconductive cadmium sulphide for a "reading matrix" involves a special problem, which has been elegantly solved by the authors.

Automatic read-out with the aid of photoresistors

With the continued advances in the field of electronic computers and their uses, it is frequently desirable to have some means by which an optical image can automatically be recognized or "read". For this purpose the image can be projected on to a plate which is prepared in such a way that the quantity of light incident on it can be determined point by point by electrical means. In cases of importance in practice, only the contour of the figure needs to be recognized, so that it is sufficient to determine which points are illuminated and which are not.

To this end, use can be made of photoresistors, e.g. of cadmium sulphide, whose electrical resistance is dependent on the intensity of illumination. A number of these photoresistors are arranged in the manner of the elements in a matrix, the image to be identified is projected on to this array, and a voltage is applied successively to each of the photoresistors. Depending on whether a large or small current begins to flow, one can conclude whether the photoresistor is illuminated or not. In order for the "reading matrix" to "see" the contour in sufficient detail, the dimensions of the picture elements, i.e. of the photoresistors employed, must be as small as possible (*fig. 1*).

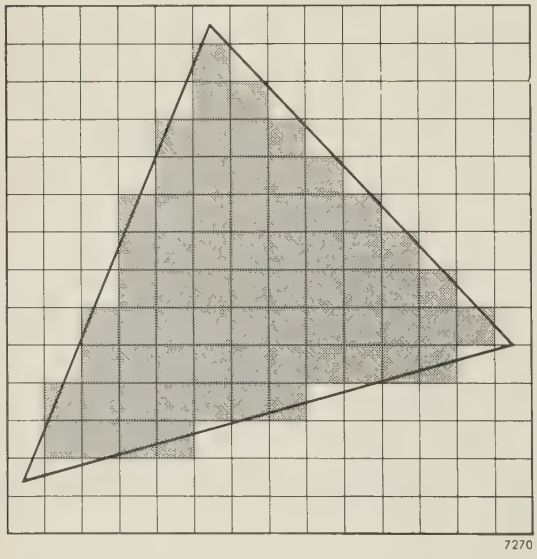

Fig. 1. How a matrix, with which an optical image can be automatically "read" (identified), "sees" the figure projected upon it.

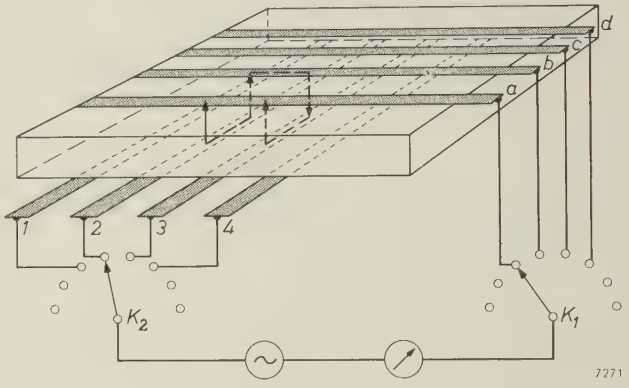

Fig. 2. Principle of automatic read-out with the aid of a matrix. On the two sides of a layer of photoconductive material, strips *a*, *b*, *c*, *d*, *1*, *2*, *3*, *4* are applied. The strips are scanned by selectors K_1 and K_2. Whenever K_1 is in one of the positions *a*, *b* . . ., K_2 traverses the positions *1*, *2*, ... When the voltage is on strips *a* and *2* and the cross-point of the strips is illuminated, a current *I* begins to flow (solid arrow). Since, as a rule, other cross points are illuminated too, stray currents flow along all sorts of paths. One of these paths is indicated in the figure by a dashed line.

The reading matrix is most simply constructed by applying conductive strips to both sides of a flat, thin layer of cadmium sulphide, as illustrated in *fig. 2*. A picture element consists of that part of the layer where two strips cross each other. (As will be explained at the end of this article, the construction of the actual array (*fig. 3*) is slightly different.) The figure to be examined is projected on to the matrix, and the strips are scanned with the aid of two selectors K_1 and K_2. Every time K_1 is in one of the positions *a*, *b*, *c*, . . . , K_2 traverses the positions *1*, *2*, *3*, ... When the position of the

*) Philips Research Laboratories, Eindhoven.

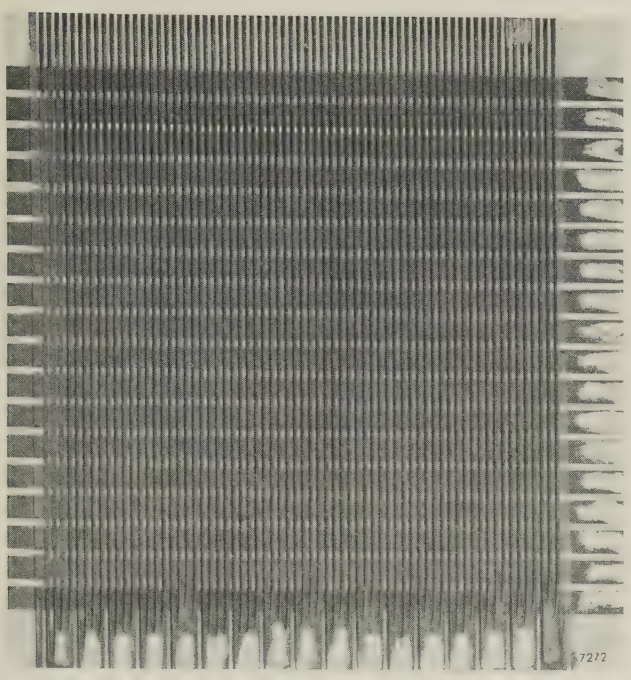

Fig. 3. A matrix for reading optical images.

selectors is such that the voltage appears on the element *a2* (between strip *a* and strip *2*), for example, a current I_{a2} starts to flow, which is higher the more light falls on *a2*. If this current is higher than a preset value, *a2* is counted as being inside the contour. The total information about the elements which is thus obtained can be compared in a computer with that for a series of contours stored in the computer memory. If the computer finds a correspondence, it reports this and the figure is recognized.

The matrix made in the manner described is not readily usable, however, for the following reason. When the voltage is across strips *a* and *2*, a current flows not only through the photoresistor *a2* but also along all sorts of other paths, e.g. through the series-connected photoresistors *b2*, *b3* and *a3*; see fig. 2. *Fig. 4* shows the equivalent circuit for a matrix containing two sets of five strips; all other resistors are seen to be in certain combinations parallel with *a2*. If there are a number of illuminated photoresistors in the parallel circuits, it is possible that stray currents will flow which will make a contribution I' to the total current I_{a2}. Thus, even though *a2* is not illuminated, the total current I_{a2} may be greater than the preset value referred to, and as a result the element *a2* is interpreted as being illuminated.

This difficulty can be overcome by using a material whose resistance depends not only on the light intensity but also on the direction in which the voltage is applied. In such a case we speak of a *photorectifier*. When the matrix is made using a material of this kind, we have what amounts to a rectifier in series with each resistor. The path for a stray current will always contain at least one rectifier in the reverse direction, so that the total contribution from the stray currents remains sufficiently low.

Although there are already a few types of photorectifiers on the market, they cannot readily be used in a matrix. This is due for one thing to their size, and for another to the fact that the matrix would have to be built up from a large number of individual elements, which would be cumbersome work compared with the application of strips to a layer. It has now proved possible, on the basis of the photoconductive material cadmium sulphide [1]), to produce a new type of photorectifier with which the matrix can easily be formed with strips in the manner described.

The new photorectifier [2])

The new photorectifier is prepared by mixing CdS powder with a small quantity of powdered

[1]) The properties and possible applications of CdS have been dealt with at length in: N. A. de Gier, W. van Gool and J. G. van Santen, Photo-resistors made of compressed and sintered cadmium sulphide, Philips tech. Rev. **20**, 277-287, 1958/59. It may be recalled here that the best photoconductive properties are obtained not with pure CdS but with powdered CdS which contains suitable additives in carefully controlled amounts. This mixture is compressed into pellets and sintered. Extremely sensitive photoresistors can be made in this way, e.g. types ORP 30, ORP 90 and LDR.B8.73104.

[2]) This photorectifier is described in: J. G. van Santen and G. Diemer, Photorectifier based on a combination of a photoconductor and an electret, Solid-state electronics **2**, 149-156, 1961 (No. 2/3), which goes into more detail.

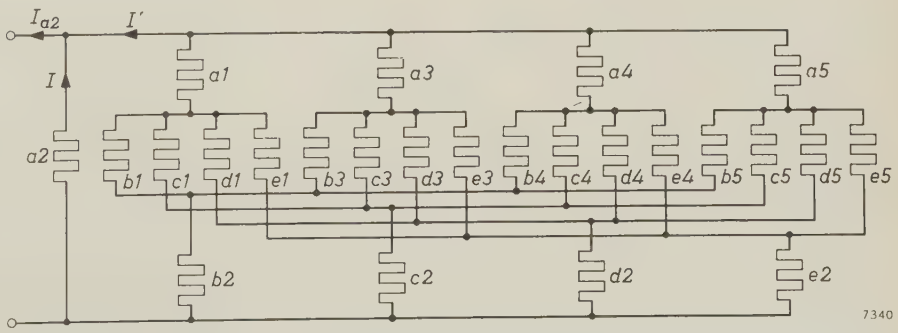

Fig. 4. When the voltage is on strips *a* and *2*, all other resistors are connected in certain combinations parallel to *a2*, as shown here for a matrix with two sets of five strips. The current I' through the parallel circuits can make such a large contribution to the total current I_{a2} as to give the impression that the element *a2* is illuminated, although it is not.

glass enamel [3]), and firing the mixture at the melting point of the enamel (about 600 °C). As a result of the adhesive forces, the enamel spreads in the form of a thin layer (thickness a few Å) between the grains (diameter a few μ), thus, as it were, cementing the grains together (*fig. 5*). Although, owing to the insulating nature of the enamel, the resistance upon illumination is considerably more than that of the sintered CdS powder, the essentially

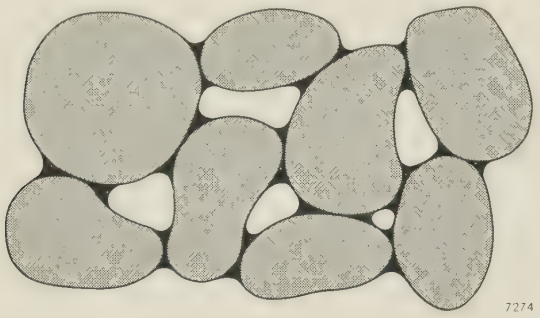

Fig. 5. Schematic cross-section of the new photorectifying material, consisting of a layer of CdS grains with glass enamel between them.

new feature is that we can now, by a special treatment, make from the enamel an *electret*, i.e. a permanently polarized dielectric, which gives the required rectification. The treatment consists in again firing the CdS and glass enamel, this time at about 200 °C, and cooling it in a strong electric field. The polarization produced in the enamel by the action of the field is thus "frozen in".

We shall now consider in more detail the explanation of the rectifying action of the combination described, and discuss its application in a matrix.

Conduction mechanism of photoconductor-electret combination

We shall first consider the case of two ordinary conductors (e.g. of copper) separated by an insulator, and discuss the conduction mechanism in terms of the band scheme as represented in *fig. 6a*, and explained in the caption to this figure *).

When a voltage is applied between the two conductors, the band schemes are mutually displaced (fig. 6*b*). Although there is now a potential difference across the insulator, no perceptible current flows, provided the insulator is not too thin. There is little chance that an electron will "tunnel" through the potential barrier *klmn*, i.e. pass from one conductor to the other without having sufficient energy to surmount the potential barrier; the probability is in fact smaller the greater are the "cross-section" *klmn* and the height *kl*. If we raise the voltage, more and more electrons will tunnel through the barrier, so that the current increases. This does not change the picture in fig. 6*b*, however, since the potential drop in the conductors is negligible. We note that the application of the voltage causes polarization in the insulator (displacement of the positive and negative charges). The accompanying additional surface charges at the contact faces between insulator and conductors are compensated by the supply and removal of the free negative charge carriers abundantly present in a conductor.

We shall now turn to the case of two grains of photoconductive CdS between which there is a very thin layer of insulating glass enamel (*fig. 7a*). When a voltage is applied to the CdS grains, the potential barrier due to the presence of the enamel undergoes a change similar to that in fig. 6*b*. Because the enamel layer is very thin, the potential barrier has a relatively small cross-section even before the

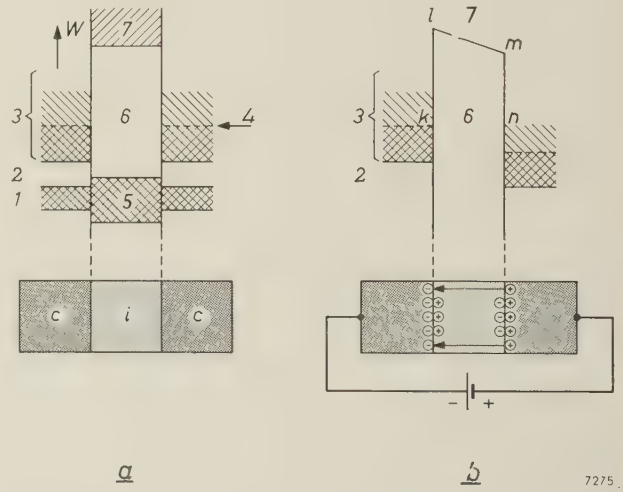

Fig. 6. *a*) Energy-level diagram showing the allowed and forbidden bands of two conductors *c* (of the same material) separated by an insulator *i*. The single hatching relates to bands of allowed levels, the cross-hatching indicates that the levels are occupied by electrons. *1* is a completely occupied band, *2* a forbidden band, *3* is the partly occupied band typical of a conductor. Some of the electrons which cannot move in the occupied levels below *4* are raised, upon the application of a voltage, to the allowed empty levels above *4*, where they can take part in the conduction. *5* and *7* are respectively a fully occupied and an empty band of the insulator, *6* is the broad forbidden band typical of an insulator: at voltages lower than the breakdown voltage the electrons cannot pass from *5* to *7*, and conduction is precluded.

Bands *1* and *5* are not drawn in *b*.

b) The application of a voltage to the conductors causes relative displacement of the band schemes. A surface charge is produced in the conductors, and partly serves to compensate the insulator surface charge, which is due to the polarization produced in the insulator by the voltage. The cross-section of the potential barrier *klmn* and the height *kl* are so large that there is hardly any chance for an electron to "tunnel" through the barrier.

[3]) Glass enamel is a type of glass which has a very short melting range (at about 600 °C), unlike normal kinds of glass, whose melting range is very long.

*) *Editor's note:* This subject will be dealt with in detail in a forthcoming article in this journal, dealing with the principles of photoconduction.

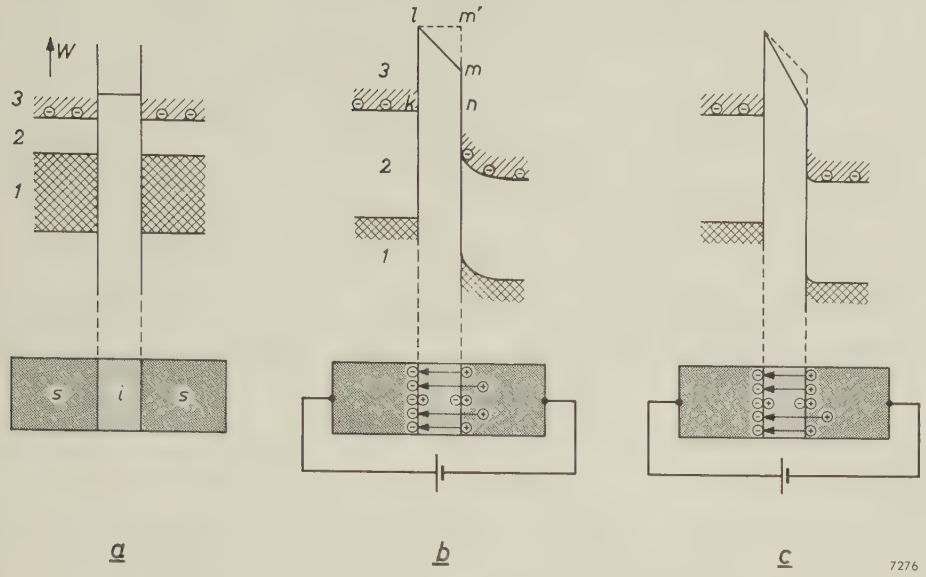

Fig. 7. *a*) The conductors in fig. 6 are replaced here by two grains *s* of photoconductive CdS; the insulator *i* is a very thin layer of glass enamel. Characteristic of a semiconductor like CdS is the forbidden band *2*, which separates the valence band *1* from the conduction band *3*. Upon absorption of a photon of sufficient energy, the electrons from the valence band can be raised to the conduction band. The relatively few electrons contained in the conduction band upon illumination are denoted here by a small number of free charge carriers and not by cross-hatching. Upon the transition of electrons from *1* to *3*, holes appear in the valence band which behave like positive charges, but which in CdS can only move slowly through the crystal lattice.
b) The already small cross-section of the potential barrier (due to the extreme thinness of the glass enamel layer) is narrowed still further when a voltage is applied. The electrons now have a greater chance to tunnel through the potential barrier, and a perceptible current flows. The holes, which are attracted towards the barrier under the action of the field, move slowly. They give rise to a space charge, and hence to a potential distribution which corresponds to a curvature of the energy levels.
c) After some time, most of the holes have reached the surface. Consequently, the potential drop is much less localized in the CdS grain than in (*b*). There is now a greater voltage across the barrier, whose cross-section is therefore still smaller. More electrons now tunnel through the barrier, as a result of which the electric current increases until a saturation value is reached. Holes constantly disappear as a result of recombination and are replaced by new holes, so that the space charge is never entirely zero.

voltage is applied. The application of the voltage narrows it still further from *klm'n* to *klmn* (fig. 7*b*). So many electrons can now tunnel through the barrier that a noticeable current starts to flow. During the first ten seconds after switching on, this current is found to be time-dependent (*fig. 8*). The reason is that the conduction mechanism in this case differs in one point from the previous one. CdS contains relatively few charge carriers, some positive and some negative. The positive charge carriers are the "holes" that are formed in the valence band when an electron jumps to the conduction band upon the absorption of a photon. These holes are not only few in number, they are also restricted in their freedom of movement by being relatively strongly bound to certain lattice sites. In the case under consideration, the holes in the positive grain also take part in the charge transport. Owing to their low mobility the holes take some time to travel to the insulator, so that there arises in the positive grain, in addition to the surface charge, a space charge near the insulator. The electrons move very fast and cause no perceptible space charge in the negative grain. Owing to the presence of the space charge, part of the potential drop is localized inside the positive grain, and this is represented by a curvature in the energy levels (fig. 7*b*). This state is not, however, stationary; more and more holes reach the surface, where they add to the surface charge. As a result the space charge decreases and the potential drop in the grain is reduced, while the potential difference across the insulator increases. The barrier becomes narrower and the current higher. After about 10 seconds a stationary state is reached. A small space charge remains (fig. 7*c*) as a result of recombination (electrons dropping back to the valence band): holes keep disappearing and fresh holes are supplied to replace them.

Summarizing then, a voltage supplied to two CdS grains gives rise to a current which rises in a time of 10 seconds to a stationary value. Its magnitude depends on the thickness of the insulator. It should be borne in mind, incidentally, that CdS is itself an insulator in the dark, when it has no electrons in the

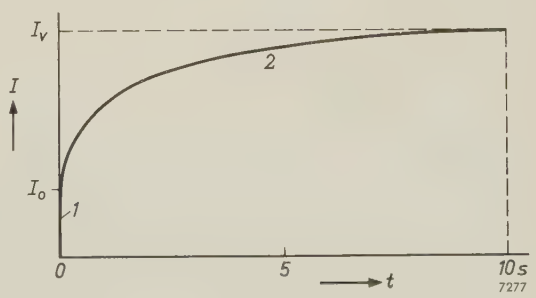

Fig. 8. The current *I* through the CdS with glass enamel, as a function of time *t* for constant voltage and illumination. The voltage is switched on at the moment $t = 0$. The curve consists of two portions: *1* immediate response, *2* slow rise to a saturation value.

conduction band. The currents mentioned are thus dependent on the illumination.

We now consider a third case, again with the two CdS grains, which are now however embedded in an electret, i.e. a thin layer of glass enamel having the above-mentioned permanent polarization. *Fig. 9a* shows the relevant band scheme. The permanent polarization in the insulator corresponds to an electric field, denoted by the arrow in the figure. The form of the potential barrier is now asymmetrical. An external voltage, applied in such a direction that the field between the grains acts in conjunction with that of the electret (fig. 9*c*), reduces the width of the barrier much more than a voltage of the same magnitude but in the opposite direction (fig. 9*b*). In the first case a current starts to flow immediately, whilst in the second case the current immediately after switching on is still almost zero.

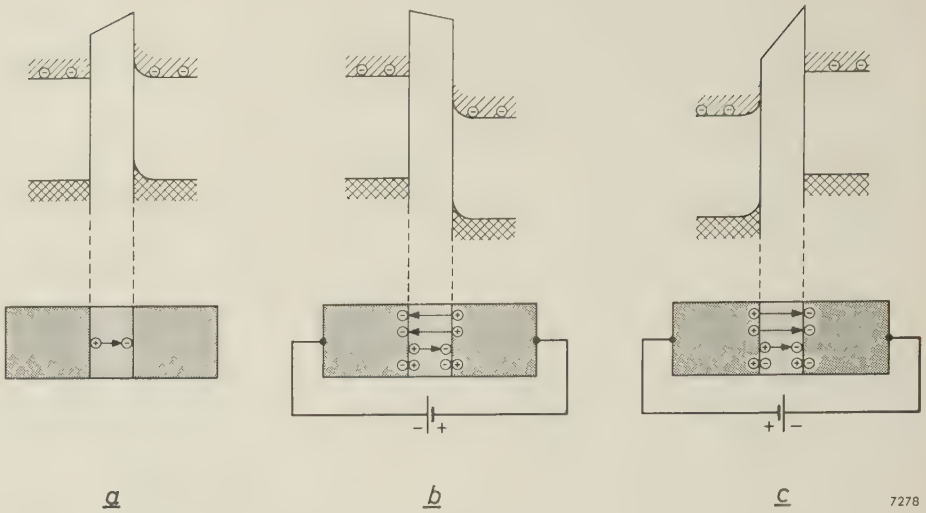

Fig. 9. *a*) The glass enamel is made into an electret by a special treatment, i.e. part of the polarization remains after the external field is removed.
b) An external voltage of the opposite polarity to that of the field of the electret is opposed by the latter field, so that the potential barrier is not significantly reduced.
c) An external voltage in the direction of the electret field makes the barrier very narrow. Immediately after application of the voltage, therefore, a much higher current flows than in case (*b*).

The above applies only *immediately after the application of the voltage*. After some time, sufficient charge carriers have arrived at the surfaces to neutralize the surface charge of the electret. The potential barrier in fig. 9*c* is then not quite so sharp, and that in fig. 9*b* is somewhat sharper, so that the two figures are each other's mirror image. The current from that moment onwards is of equal magnitude in both cases. *Fig. 10* shows the difference between the currents in the two directions as a function of time.

Now it follows from fig. 10 that the resistance of illuminated CdS with glass enamel is equal in both directions upon the application of direct voltage (at least after 10 seconds), *but upon the application of alternating voltage it is greater in one direction than in the other*. For alternating currents, the system is always in the state prevailing immediately after switching on. The combination CdS-electret-CdS is thus seen to have a rectifying action for alternating current. A current-voltage characteristic of this new rectifier can be seen in *fig. 11*.

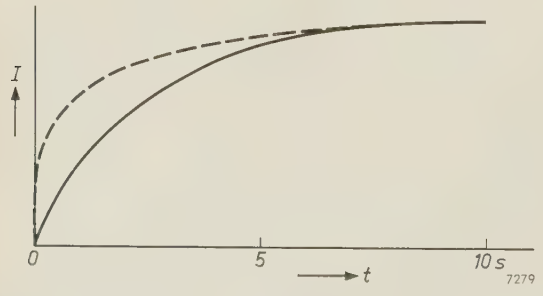

Fig. 10. Photocurrent I in CdS with polarized enamel as a function of time t, in the forward direction (broken curve) and in the reverse direction (solid curve). In the forward direction part of the response is immediate, but not in the reverse direction.

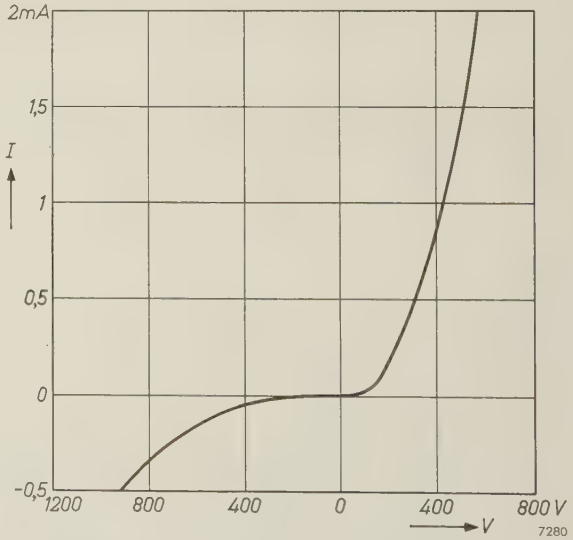

Fig. 11. Current-voltage characteristic of CdS with polarized enamel, for alternating voltage. All frequencies above about 1 c/s give the same curve.

Application of the photorectifier material in a reading matrix

To give an impression of the effect of illumination, *fig. 12* shows the relation between current and voltage for CdS with unpolarized enamel, subjected to

various intensities of illumination. For comparison, the figure includes a curve relating to sintered CdS powder [1]). It should be remembered in this connection that, apart from the photoconductive properties of the two materials, a part is also played by other factors such as the interelectrode spacing and

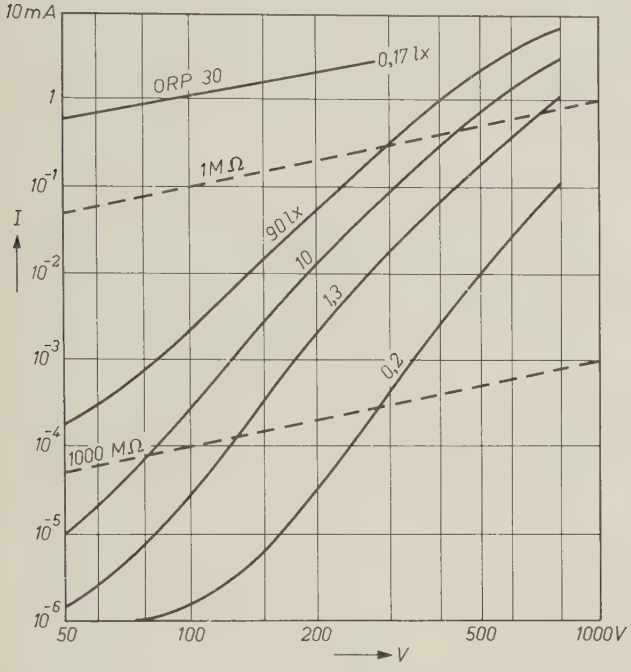

Fig. 12. Current-voltage characteristics of the photoconductive CdS layer with unpolarized enamel, illuminated with 0.2, 1.3, 10 and 90 lux respectively, and of sintered CdS powder (ORP 30) illuminated with 0.17 lux. The dashed lines apply to normal resistors of the value indicated. The relation between I and V for the CdS layer with enamel is approximately given by $I \propto V^5$, and its resistance is roughly a factor of 10^6 greater than that of sintered CdS.

the surface area exposed to the light [2]). Even so, it is reasonable to deduce from fig. 12 that the sintered CdS powder has a *small* and *constant* resistance, whereas the resistance of CdS with enamel is much *higher* for the same illumination, and is moreover *dependent on the voltage*. This is bound up with the fact that the resistance is primarily governed by the form of the potential barrier and not by the CdS.

Fig. 12 shows that the illumination can easily reduce the resistance of CdS with glass enamel by a factor of 1000. The material can thus be used for a reading matrix as described in the introduction. The obstacle to the discrimination between light and dark due to stray currents (fig. 2) is now overcome by the rectifying effect: when the voltage is applied in the forward direction to one particular photoresistor, there will then, as explained above, be rectifiers in the reverse direction in all other possible paths.

Fig. 13 represents a cross-section of a matrix as actually made. The grooves between the upper strips are applied for the following reason. The photons cannot penetrate deep into the material, so that the photoconduction takes place primarily near the surface. When the photoconductive material is grooved in the manner illustrated, the current is able to flow from an upper strip to a lower one via the surface layer. Without this grooving, the resistance in the forward direction would be too high.

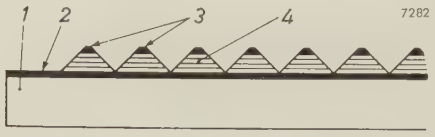

Fig. 13. Cross-section of an actual matrix. *1* ceramic base. *2*, *3* electrode strips. The photoconducting layer *4* of CdS embedded in glass enamel is deeply grooved.

One last comment on this resistance. For practical applications, the relatively high resistance is a drawback. Because of the voltage dependence mentioned (fig. 12), however, we can make the resistance quite a lot smaller by choosing a higher voltage. If the matrix is used in conjunction with equipment containing electron tubes, this presents no difficulty. Since the advent of the transistor, however, there has been a tendency to work with low voltages (below 40 V), and in that case the resistance of each element of the matrix would be too high. This difficulty can be met by choosing the highest feasible value of illumination and by designing the matrix so that every picture element always contains a number of photorectifiers, e.g. four, in parallel, thus reducing the resistance per element by a factor of 4. (The matrix in fig. 3 was designed in this way, the upper strips being divided into three.) This conflicts of course with the requirement that the elements should be as small as possible in order to allow accurate read-out, so on this point a compromise has to be accepted.

Summary. The simplest way of making a matrix with which an optical image can automatically be read (identified) is by applying parallel conducting strips to both sides of a thin layer of photoconductive cadmium sulphide, in such a way that the strips on one side cross those on the other side at right angles. This "cross-bar" construction entails stray currents, which hinder the discrimination between light and dark. A new photorectifying material is described, which is based on a combination of a photoconductor (CdS) and an electret (i.e. a permanently polarized glass enamel). When the ordinary CdS is replaced by this photorectifying material, the stray currents are largely suppressed. The rectifying effect in this material can be satisfactorily explained with the aid of the energy-band model.

DISPENSER CATHODES FOR MAGNETRONS

by G. A. ESPERSEN *).

621.3.032.213.2:621.385.16

The use of dispenser cathodes such as the L cathode or the impregnated cathode offers great advantages in magnetrons, klystrons and other tubes. Millimetre-wave magnetrons and high-power continuous-wave magnetrons for centimetre waves using these cathodes can attain a life of 1000-3000 hours. The operation is moreover very stable, and long pulses can be used.

Comparison of dispenser cathodes with oxide-coated cathodes

Most of the *oxide-coated cathodes* used in magnetrons have a porous nickel matrix. In the manufacture of these cathodes, a layer of nickel powder a few tenths of a millimetre thick is sintered on to a nickel cylinder. This porous layer is then covered with a paste of the emitting material, usually a mixture of $BaCO_3$ and $SrCO_3$, which is later converted to the oxides by heating. The object of this porous layer of metal is to reduce the voltage drop across the oxide layer, which may occur when large pulsed currents are used. If this voltage is high, breakdown may occur locally, leading to the emission of incandescent oxide particles (sparking) or the production of a visible gas discharge (arcing).

Oxide-coated nickel-matrix cathodes give excellent performance in most pulse-type magnetrons if the cathode temperature does not exceed 900 °C. It has however been found that oxide-coated cathodes have very short lives when used in millimetre-wave magnetrons, where high cathode current densities are required, and in high-power continuous-wave magnetrons, where the cathode operates at temperatures in excess of 900 °C.

It has therefore become the practice in recent years to replace the oxide-coated cathode by a *dispenser cathode* in such magnetrons. This dispenser cathode may be an L cathode [1]) or an impregnated cathode [2]). The smooth surface of the dispenser cathode ensures its ability to operate at high temperatures with relatively few arc breakdowns. This may be clearly seen from *fig. 1*, which shows the number of discharges per minute as a function of time for a 22-kW pulsed-type magnetron for the 3-cm band (type PAX-6) with an oxide-coated cathode (*a*) and for one with an L cathode (*b*) [3]). Each breakdown is moreover much less dangerous in the dispenser cathode than in the oxide-coated cathode, since the body of the former is composed entirely of tungsten and molybdenum, which have very high melting points (above 2600 °C). It is noted that the cathode temperature of both the oxide-coated matrix and the L-type cathodes in these arcing studies was approximately 950 °C and it is believed that under these conditions considerable nickel vaporization of the oxide-coated matrix cathode took place, resulting in the excessive number of arc counts.

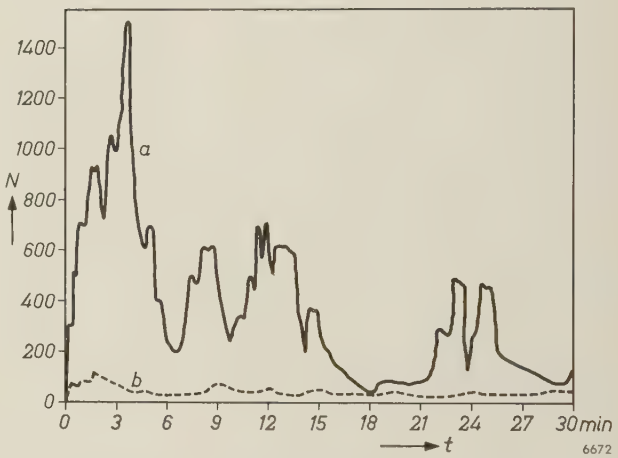

Fig. 1. Number of discharges per minute, N, as a function of the time t in a PAX-6 tube (200 pulses per sec of 5 μsec, 15 kV and 16 A), *a*) with oxide-coated cathode, *b*) with L cathode.

Another advantage of the use of the dispenser cathode in magnetrons is that for a given repetition rate it can be operated at much longer pulse lengths than the oxide-coated cathode. This has been investigated using 70-kW pulsed-type magnetrons for the 3-cm band (type 6507). In operating these tubes at the rated value of duty factor (0.001) the cathode

*) Philips Laboratories, Irvington-on-Hudson, N.Y., U.S.A.

[1]) H. J. Lemmens, M. J. Jansen and R. Loosjes, A new thermionic cathode for heavy loads, Philips tech. Rev. **11**, 341-350, 1949/50.

[2]) R. Levi, Philips tech. Rev. **19**, 186-190, 1957/58.

[3]) Most of the experiments mentioned here have already been described in: G. A. Espersen, Dispenser cathode magnetrons, I.R.E. Trans. on Electron Devices **ED-6**, 115-118, 1959.

temperature is 775 °C with the heater turned off. Under these conditions, tubes with oxide-coated matrix cathodes and with dispenser cathodes have comparable performance. If the pulse length (and hence the duty factor) is increased about threefold, the cathode temperature increases to 950 °C and the tubes with oxide-coated cathodes show considerable plate-current instability (*fig. 2a*), while the tubes with dispenser cathodes show little or no instability (fig. 2*b*). This difference was also found with tubes of other types.

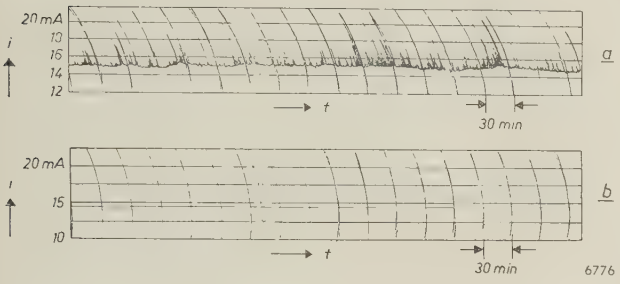

Fig. 2. Anode current i recorded as a function of the time t for a 6507 tube, *a*) with oxide-coated cathode, *b*) with impregnated cathode.

The construction of the cathode

The cathodes of magnetrons are nearly always cylindrical. *Fig. 3* shows typical constructions for the L cathode (*a*) and the impregnated cathode (*b*). The impregnated cathode has various advantages over the L cathode, e.g. a simpler structure with better thermal efficiency, more homogeneous temperature distribution along the emitting area, no need for a gas-tight weld, and more rapid evacuation. Moreover, when the external dimensions of the two types are the same, the impregnated cathode has more room for the heater (*2* in fig. 3). A heater having a larger surface area may be used and consequently it can be operated at a lower temperature to obtain the same temperature of the emitting body. This is an important advantage, especially as the temperature of the emitting body of a dispenser cathode must be higher than that of an oxide cathode in order to give the same emission.

Breakage of the heater filament is in fact the main cause of the failure of dispenser cathodes in a magnetron; the filament must therefore be designed with the greatest care. The insulating layer of aluminium oxide which is found on the heaters of oxide-coated cathodes is often omitted in dispenser cathodes because aluminium oxide reacts with the tungsten at high temperatures. The heater must then not touch the inside of the cathode at any point. As may be seen in fig. 3, a ring of ceramic aluminium oxide (*3*) is used, on one end of the cathode, for centering and insulation; but this is not in direct thermal contact with the heater.

The holder for the porous tungsten cylinder is made of molybdenum, and is brazed to the tungsten with a eutectic mixture of nickel and molybdenum at 1400 °C in an atmosphere of hydrogen.

The cathode is "seasoned" during the evacuation of the tube, i.e. the heater voltage and anode voltage are applied, so that the cathode passes current. This process is completed more quickly with dispenser cathodes than with oxide-coated cathodes, because the latter have more sharp points and other irregularities on the surface which must be burnt away. Care must be taken that the temperature of the dispenser cathode remains as low as possible, preferably below 1150 °C, in order to achieve optimum life, ensure coverage of the cathode surface by a full barium monolayer and to prevent "end emission". This very undesirable effect will now be discussed.

End emission

The magnetron has a high efficiency because the electrons can reach the anode only when their potential energy is mainly used for maintaining the

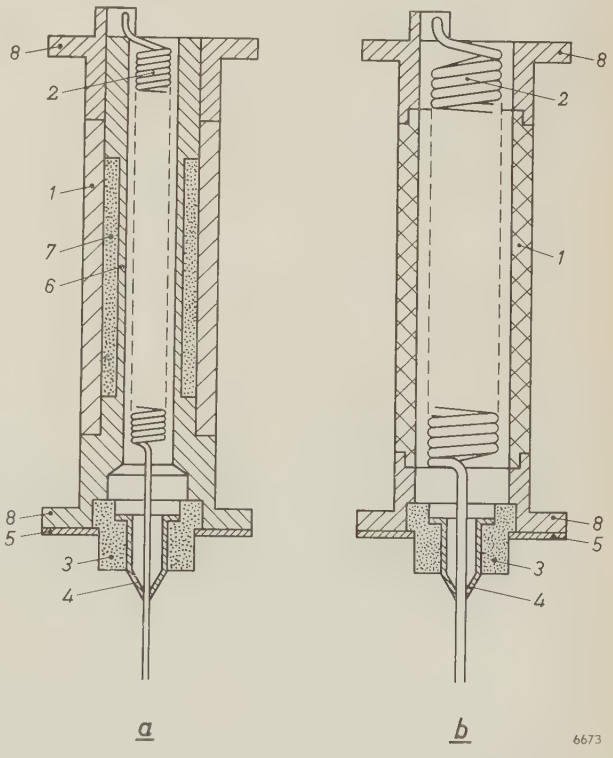

Fig. 3. Sketch of *a*) L cathode, *b*) impregnated cathode. In both figures, *1* is the porous tungsten cylinder, *2* the heater, *3* the aluminium-oxide insulation for the heater, *4* a tantalum eyelet and *5* a tantalum washer. *6* is the molybdenum inner cylinder in *a*), *7* is the emitting material in *a*), and *8* are the molybdenum end shields. In *b*) the tungsten cylinder is impregnated with the emitting material.

HF electric field. The axial component of the velocity of the electrons could however lead to a considerable current loss between the cathode and the anode. The cathode is therefore provided with end shields (fig. 3) which give rise to a field which forces the electrons back into the space between the cathode and the anode. If however the end shields themselves emit, these electrons can proceed in an axial direction, e.g. to the pole pieces, causing a decrease in the efficiency.

End emission can be caused by evaporation and/or migration of the emitting substance from the cathode proper. This can be prevented in a number of ways, in the first place by keeping the cathode temperature as low as possible. This is especially important during the seasoning of the cathode, as has already been mentioned above. It is however never possible to prevent migration and evaporation of the emitting substance at the temperatures needed for emission, at least with the dispenser cathode. We are thus left with the possibility of choosing the material and the construction of the end shields so that their temperature is kept as low as possible and so that they emit as little as possible when the emitting substance is deposited on them.

Fig. 4 shows a construction which considerably lowers the temperature of the ends by surrounding them with cylindrical screens about 1 cm long, and with a wall thickness of 0.25 mm. If the cathode temperature is 1185 °C at point *C*, the temperature at the points *B* and *D* on the screens is 1025 °C if molybdenum is used for making the latter and only 900 °C if tantalum is used. The end shields of the cathode shown in fig. 3 (which are 0.5 mm thick) had a temperature of 1110 °C under the same conditions. Titanium is also a suitable material for the screens: it has a low thermal conductivity and low thermal emission [4]), and has a gettering effect, but it can only be used if its temperature does not exceed 800 °C. Zirconium likewise has low emission and a gettering effect. Tantalum and titanium, however, present a difficult brazing problem; the same is true for zirconium, which moreover recrystallizes under the operating conditions as may be clearly seen from *fig. 5*. Zirconium-coated molybdenum screens were therefore adopted for the final design of the 5780 A 3-cm magnetron [5]).

A measure of the end emission is given by the anode current of the magnetron with a much reduced voltage, in the presence of the magnetic field. The tube does not oscillate under these conditions and the current then comes mainly from the ends of the cathode. A tube which normally operates at an anode voltage of 32 kV and an anode current of 40 A

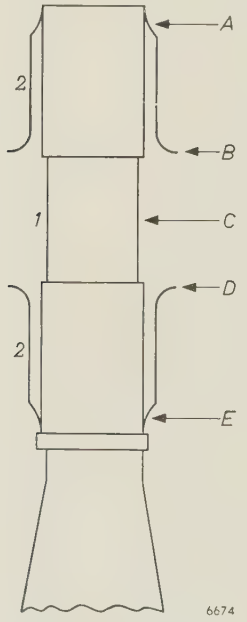

Fig. 4. Special construction of magnetron cathode to reduce end emission. *1* cathode, 7.6 mm in diameter and 8.2 mm long. *2* peripheral construction, 9.4 mm long and 0.25 mm thick.

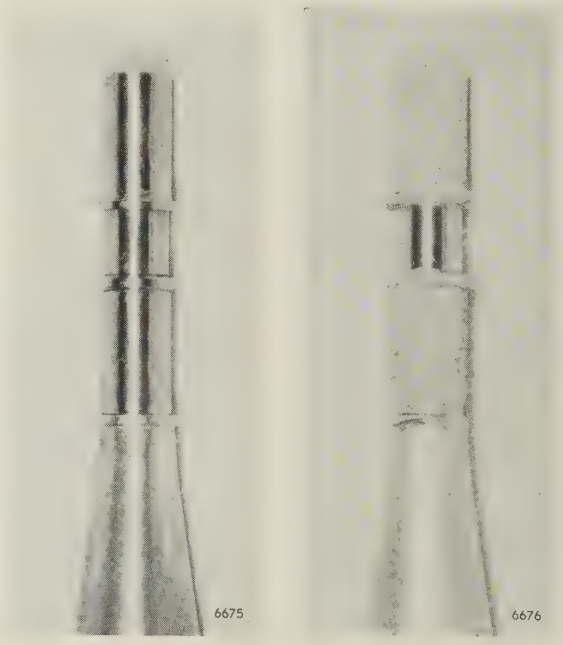

a *b*

Fig. 5. Cathode with zirconium screens, *a*) before seasoning, *b*) after 280 hours' life testing.

[4]) G. A. Espersen and J. W. Rogers, Philips tech. Rev. **20**, 269-274, 1958/59.

[5]) A new technique for suppressing the electron emission from portions of tungsten dispenser cathodes consists in carburizing the areas to be rendered non-emitting by completely covering them with finely divided graphite and heating at a temperature of 1500 to 1800 °C in an atmosphere of hydrogen for a period of 5 to 15 minutes. See R. Levi and E. S. Rittner, Proc. Inst. Radio Engrs **49**, 1323, 1961 (No. 8).

Table I. Life data of magnetrons with dispenser cathodes.

Type	Sort of cathode	Frequency	Operating conditions						Mean life
			pulse or continuous	anode voltage	anode current	power	duty factor	pulse length	
		(Gc/s)		(kV)	(A)	(kW)		(μs)	(h)
DX 107 A	imp.	3.4	pulse	28	50	500	0.0005	4.0	960
PAX-6	L	9.4	pulse	15	7	22	0.0023	4.65	650
PAX-6	imp.	9.4	pulse	15	7	22	0.0023	4.65	670
6507	imp.	9.4	pulse	16	15	70	0.001	1.0 and 5.0	690
6507	imp.	9.4	pulse	16	15	70	0.001	15.0	1080
7093	imp.	35.0	pulse	15	16	32	0.0003	0.5	1500
DX 164	imp.	75.0	pulse	13	10	25	0.0002	0.1	200
7091	imp.	2.4	cont.	4.5	0.75	2.0	—	—	3000
7292	imp.	2.4	cont.	4.5	0.75	2.0	—	—	3000

may e.g. be given an anode voltage of 10 kV for this measurement. The anode current measured on one particular tube in this way was 1.0 mA for the unused tube, 2.5 mA after 1000 hours and 5.0 mA after 5000 hours.

Secondary emission

It is known that a large part of the current in oscillating magnetrons may be supplied by secondary emission, due to electrons which are accelerated by the RF field in the cathode-anode space and return to the cathode along a curved path. For example, an oscillating magnetron can give a peak anode current of 16 A and at a cathode temperature corresponding to a (primary) saturation current of 100 mA. Such an extreme case is not favourable, because the current can easily become unstable, but a certain supplementation of the primary emission by secondary emission is desirable. The secondary-emission coefficient, i.e. the number of secondary electrons produced per incident electron, is greatest for an oxide-coated cathode, other things being equal, and it is greater for an impregnated cathode than for an L cathode. Even an L cathode, however, has a secondary-emission coefficient greater than unity under normal conditions [6]), so use can still be made of the secondary emission.

[6]) I. Brodie and R. O. Jenkins, Brit. J. appl. Phys. **8**, 202-204, 1957.

Life

Life tests were carried out on a number of magnetrons of four different types. The results are summarized in *Table I*. The reason for failure was nearly always a broken heater. Types 7091 and 7292 differ from each other only in the anode cooling system. The 3-cm types mentioned in this table have recently been superseded by the types 7008, 7110, 7111 and 7112, which have a mean life exceeding 1000 hours and are considerably more stable, showing less jitter for short pulses.

It may be seen from the table that the life of these magnetrons can be much longer than that of magnetrons with oxide-coated cathodes, which usually lies between 50 and 500 hours. The long life of types 7091 and 7292 is especially important, as they are used in cooking ovens [7]), where the price of the magnetron is an important part of the cost of the whole installation.

[7]) W. Schmidt, The heating of food in a microwave cooker, Philips tech. Rev. **22**, 89-102, 1960/61 (No. 3).

Summary. The use of dispenser cathodes in magnetrons of a number of types is described. A cylindrical cathode offers only limited room for the heater, which necessitates special heater constructions. End emission, which is very undesirable in magnetrons, can be reduced by giving the edges of the cathode a low thermal conductivity and low emission. The results of a number of life tests on magnetrons indicate that those with dispenser cathodes last much longer than those with oxide-coated cathodes. Moreover, tubes with dispenser cathodes are much more stable and can withstand longer pulses.

ABSTRACTS OF RECENT SCIENTIFIC PUBLICATIONS BY THE STAFF OF N.V. PHILIPS' GLOEILAMPENFABRIEKEN

Reprints of those papers not marked with an asterisk * can be obtained free of charge upon application to the Philips Research Laboratories, Eindhoven, Netherlands, where a limited number of reprints are available for distribution.

2896*: J. D. Fast: Entropie. Die Bedeutung des Entropiebegriffes und seine Anwendung in Wissenschaft und Technik (Philips Technical Library, 1960, XII+328 pp., 68 figures, 26 tables). (Entropy. The significance of the concept of entropy and its applications in science and technology; in German.)

A German translation of a Dutch book. The English translation will be published in the course of this year, and will be more fully reviewed.

2897*: H. G. van Bueren: Imperfections in crystals (North-Holland Publishing Co., Amsterdam 1960, XVIII+676 pp.).

This book is written mainly for solid-state physicists who are interested in the effect of imperfections in the crystal lattice on the properties of the material they are investigating. A large number of properties of the solid state are discussed, together with the role imperfections play in determining these properties. Considerable attention is paid to the theoretical interpretation of the phenomena in question, and their interrelation. The book is divided into three parts, which deal with: the general properties of imperfections in crystals (4 chapters, 110 pp.), the metals (19 chapters, 400 pp.) and the non-metals (8 chapters, 143 pp.). The lists of references at the end of the various chapters contain in all about 1000 items.

2898: E. E. Havinga: Contribution to the theory of the dielectric properties of the alkali halides (Phys. Rev. **119**, 1193-1198, 1960, No. 4).

In this paper some relations between dielectric properties of diagonal cubic ionic crystals are derived on the basis of the Dick and Overhauser shell model for ions. The relations, which contain no model constants, are in good agreement with experimental data. Also it is shown that Dick and Overhauser overestimated the number of electrons in the shells of the ions, which accounts for the failure of their quantitative treatment. In an appendix the paper of Hanlon and Lawson on the same subject is discussed.

2899: H. Bremmer: On the theory of wave propagation through a concentrically stratified troposphere with a smooth profile (J. Res. Nat. Bur. Standards **64 D**, 467-482, 1960, No. 5).

The Wentzel-Kramers-Brillouin approximation for the solution of the height-gain differential equation for a curved stratified troposphere is discussed in detail. The approximation depends mainly on a variable $u_1(r)$ which can be interpreted as the height-dependent contribution of the phase for a field solution obtained by separation of variables. An expansion of $u_1(r)$ with the aid of partial integration leads to further approximations which facilitate the determination of the eigenvalues, and of the amplitudes of the modes connected with the propagation problem. The influence of the refractive-index profile, if assumed as smooth, then appears to be restricted to a dependence on the surface values of this index and of its gradient insofar as propagation over the ground is concerned. Further, all height effects of elevated antennas can be expressed in terms of the distance to the corresponding radio horizon. This results in simple relations between the fields connected with two different refractive-index profiles, provided both profiles coincide near the earth's surface.

2900: W. Black, J. G. V. de Jongh, J. Th. G. Overbeek and M. J. Sparnaay: Measurements of retarded Van der Waals' forces (Trans. Faraday Soc. **56**, 1597-1608, 1960, No. 11).

Molecular attractions are measured between pairs of flat quartz plates and between a flat and a spherically curved plate. Considerable precautions are taken against spurious electric charges, dust and gel particles which might interfere with the measurements. Silicone oil is used for damping. Distances between the flat plates have been varied from 5000-9500 Å, and from 940-5000 Å for the plate and sphere combination. Attraction forces varied from 0.002-0.3 dyne. The results agree with the presence of retarded Van der Waals' forces (Casimir and Polder, Lifshitz). If the force per unit area between flat plates is represented by $F = -B/d^4$, the value of B, which is $1\text{-}2 \times 10^{-19}$ erg cm, is in good agreement with exist-

ing theories, and with the previous experimental results obtained by Derjaguin and Abrikosova and by Kitchener and Prosser. An explanation is suggested why earlier measurements by Overbeek and Sparnaay using a similar method led to much stronger attractions.

2901: S. Duinker and B. van Ommen: The scansor, a new multi-aperture rectangular-loop ferrite device (Solid-State Electronics **1**, 176-182, 1960, No. 3).

The scansor consists of a multi-aperture plate of rectangular-loop ferrite material which is provided with a large number (e.g. 10-20) of separate output windings across which consecutive output pulses can be developed by driving the plate from one remanence position into the other by triangular-shaped pulses. The various output pulses are of rather uniform height but mutually delayed. Depending on the geometry of the scansor and on the slope of the driving current, the delay between pulses corresponding to any two adjacent single-turn output windings can be varied from 0.05 to 2 μs with corresponding pulse heights of 10 to 0.2 V. Experiments are described showing that the response of certain output windings can be either suppressed or shifted in time by applying appropriate additional pulses. A few possible applications of scansors such as rapid scanning devices and code converters are briefly discussed.

2902: C. M. van der Burgt: Piezomagnetic ferrites — applications in filters and ultrasonics (Electronic Technol. **37**, 330-341, 1960).

A survey of the properties and possible applications of ferrites with a high magnetostrictive effect, in particular of the recently developed Ni-Cu-Co ferrites. The conditions which these materials must satisfy for use in high-power transducers (devices for transforming electrical energy into mechanical and *vice versa*) are discussed, as are the conditions for use in electro-mechanical band-filters. Some details of such band-filters are also given. Special attention is paid to the use of such transducers for cleaning small objects by means of ultrasonic vibrations in a liquid. A self-oscillating ultrasonic drill for use with brittle materials is also described; with a few modifications, this could also be used as a self-oscillating ultrasonic welder. All these piezomagnetic transducers can incorporate feed-back elements made of piezo-electric ceramic materials.

2903: U. Enz: Spin configuration and magnetization process in dysprosium (Physica **26**, 698-699, 1960, No. 9).

Dysprosium is ferromagnetic below 85 °K and has some type of antiferromagnetic structure between 85 °K and 178.5 °K, the Néel temperature. It is shown in this paper that the magnetic properties of Dy in the antiferromagnetic region can be completely understood by assuming a helical spin configuration. The period of the helix is a function of the temperature. The behaviour of a helical spin configuration in a magnetic field is calculated.

2904: H. C. Hamaker: Le contrôle qualitatif sur échantillon (Rev. Statistique appl. **8**, No. 2, 5-40, 1960). (Quality control by sampling; in French.)

The fundamental principles forming the basis of sampling inspection are reviewed in this article. The theory of operating-characteristic curves is first examined briefly. The aims of sampling inspection procedures and the various factors to be considered are then enumerated and discussed. In the following sections economic theories, the distribution of percentage rejects in inspected batches and the relation between batch size and sample size are studied in some detail. In particular, emphasis is laid on the importance in many industrial problems of the use of samples of constant size, independent of the batch size.

In the second part of the article the special characteristics are examined of the various sampling tables in common use on both sides of the Atlantic. They are compared from various points of view: specifications of the quality, relations between size of sample and quality and between sample size and batch size, stringency of inspection, simple and double sampling, range of scales and general aspects. In a final section the author presents the characteristics that he considers desirable in a sampling procedure.

2905: B. G. van den Bos: Investigations on pesticidal phosphorus compounds, II. On the structure of phosphorus compounds derived from 3-amino-1,2,4-triazole (Rec. Trav. chim. Pays-Bas **79**, 836-842, 1960, No. 8).

A previous publication (No. **2883**) described pesticides obtained e.g. by reaction of 3-amino-1,2,4-triazole (or a 5-substituted derivative thereof) with *bis*(dimethylamido) phosphoryl chloride. It is shown in the present publication that the phosphoryl group in these compounds is attached to the triazole ring. The preparation of a number of compounds involved in this investigation (in collaboration with A. J. Visser and K. Wellinga) is described in the experimental part.

2906: H. J. L. Trap and J. M. Stevels: Conventional and invert glasses containing titania. Part 1 (Phys. Chem. Glasses **1**, 107-118, 1960, No. 4).

An investigation of some properties of conventional and invert glasses containing titania. The viscosity and thermal expansion of such glasses do not differ from those of glasses which do not contain titania, but their electrical properties do. The phenomena observed are related to two effects: 1) reinforcement of the structure of the glass by Ti^{4+} ions (mainly in conventional glasses), and 2) the formation of sub-microscopic regions rich in TiO_2 (mainly in invert glasses). The Ti^{4+} ions act as network-modifying ions, not as network-forming ions. They give rise to closer packing, and thus to anomalous variation of the dielectric constant. The effect of these ions is reduced by the presence of Pb^{2+} ions. The presence of Ti^{4+} ions gives rise to attractive properties in both conventional and invert glasses. See also Philips tech. Rev. **22**, 300, 1960/61 (No. 9/10).

2907: C. Jouwersma: On the theory of peeling (J. Polymer Sci. **45**, 253-255, 1960, No. 145).

A critical discussion of an equation derived by Bikerman for the force needed to pull a glued layer loose from a flat surface. With the aid of improved boundary conditions, an equation which agrees better with the experimental results is derived. The degree to which the glue may be regarded as following Hooke's law is also discussed.

2908: F. J. Janssen: An electronic spirometer (Proc. 2nd int. Conf. on medical electronics, Paris, June 24-27, 1959, pp. 339-340, Iliffe, London 1960).

Brief extract from an address delivered at the above-mentioned congress, dealing with an electronic method of measuring the volume of air displaced during respiration.

2909: W. J. Oosterkamp: Nieuwe mogelijkheden voor de röntgendiagnostiek (J. belge Radiol. **43**, 379-385, 1960, No. 4). (Advances in X-ray diagnostic techniques; in Dutch.)

The main idea behind the development of new X-ray equipment in the Philips laboratories is how to get more information with smaller doses. With this aim in mind, the author discusses: an X-ray image intensifier with a screen 23 cm (9 inches) in diameter, a closed-circuit television system for observing the image formed by the image intensifier, and a magnetic memory for recording X-ray images. Although economy in the use of radiation is recognized to be important, this economy must not be at the expense of image quality. Even in the future, full-size pictures will be indispensible where the utmost image quality is required.

2910: H. F. L. Schöler: Biological properties of 9,10-isomeric steroids, I. Progestational activity of $9\beta,10\alpha$-steroids (Acta endocrinol. **35**, 188-196, 1960, No. 2).

The progestative effect of four steroids with the $9\beta,10\alpha$ structure was compared with that of progesterone by means of the Clauberg test. The four compounds investigated, retro-progesterone, 6-dehydro-retro-progesterone, 17α-acetoxy-retro-progesterone and 6-dehydro-17α-acetoxy-retro-progesterone were effective whether administered orally or subcutaneously. The maximum effect (compared with 10 mg progesterone subcutaneously) was obtained by subcutaneous administration of 5, 1, 1 and 0.5 mg respectively, or by oral administration of 50, 10, 2.5 and 1.25 mg respectively. See also these abstracts, Nos **2881** and **2882**.

2911: G. W. van Oosterhout: Morphology of synthetic submicroscopic crystals of α and γFeOOH and of γFe_2O_3 prepared from FeOOH (Acta crystallogr. **13**, 932-935, 1960, No. 11).

The orientation of the needle axis of synthetic acicular crystals of α and γFeOOH with respect to the unit cell has been determined by selected-area electron diffraction. The needle axis is [001] for αFeOOH ($c = 3.03$ Å) and γFeOOH ($c = 3.06$ Å) and [110] for γFe_2O_3 prepared either by dehydration of γFeOOH or by reduction of αFeOOH or γFeOOH followed by oxidation.

The results are compared with previous work on this subject and the possible causes of the discrepancies between the results of Osmond and of Campbell and those obtained in the present paper are discussed.

2912: J. M. Stevels: Network defects in non-crystalline solids (Conf. non-crystalline solids, Alfred (N.Y., U.S.A.), Sept. 1958, pp. 412-448, Wiley, New York 1960).

After a survey of the present theories about the structure of glass, in particular quartz glass, the author discusses the information that can be gained about the structure from measurements of dielectric losses at high and low temperatures and from the effect on the optical absorption spectrum of exposure to ultraviolet light, X-rays, γ-rays and neutrons. The measurements of dielectric losses show promise of allowing us to distinguish between five ways in

which ions and electrons can move in glass, quartz glass and quartz. Combination of these measurements, particularly those at low temperature, with measurements of the optical absorption and paramagnetic resonance allow a number of network defects in glass and quartz to be recognized and identified. These methods can also sometimes yield information about local crystallization in glass or local vitrification in quartz crystals. In a number of cases the effect of irradiation can be described by a sort of chemical equation ("operational equation").

2913: J. Rodrigues de Miranda: Photo-sensitive resistor in an overload-preventing arrangement (IRE Trans. on Audio **AU-8**, 137-139, 1960, No. 4).

Description of a device for preventing overloading of an amplifier. The pre-amplified signal is fed via a voltage divider to the input of a high-power amplifier. The voltage divider contains a photo-sensitive resistor (CdS). The output of the amplifier feeds a neon lamp, which is situated together with the photo-resistor in a light-proof box. The neon lamp begins to burn as soon as the voltage exceeds a certain limiting value. The input signal is thus attenuated, making overloading impossible.

2914: G. Diemer: Nature of an ohmic metal-semiconductor contact (Physica **26**, 889, 1960, No. 11).

The author clarifies some assumptions made in a previous publication about the nature of the contact between an indium electrode and a crystal of *N*-type CdS. The indium probably diffuses along dislocations etc. into the CdS, forming "spikes" of much lower resistivity than the surrounding crystal. The current will then spread from these spikes throughout the crystal, giving rise to an ohmic voltage drop near the electrodes.

2915: H. G. van Bueren: The flow stress of germanium crystals (Physica **26**, 997-999, 1960, No. 11).

The author has previously published an expression for the creep velocity of germanium crystals which implicitly involves the velocity v of dislocations. The exponential relationship between the creep velocity on the one hand and the tensile stress and temperature on the other can be explained from the way v varies with these quantities. This view contradicts the results of Haasen and Alexander to a certain extent. An attempt is made in the present publication to extend the theory so as to eliminate this contradiction.

2916: M. J. Sparnaaij: Electro-osmosis experiments at the germanium/electrolyte interface (Rec. Trav. chim. Pays-Bas **79**, 950-961, 1960, No. 9/10).

Measurements of the electro-osmotic fluid transport in a mixture of Ge powder and an electrolyte. In analogy with a theory of Verwey and Payens (originally developed for surface layers of weakly ionized fatty acids) it is assumed that the surface-oxidized Ge is surrounded by a layer of H_2GeO_3 or some other acid when it is in contact with an aqueous solution. This acid yields up hydrogen ions to the solution, while the $HGeO_3^-$ residues are adsorbed on the semiconductor, giving rise to a surface charge which is responsible for the observed phenomena. The difference in behaviour between *P*-type and *N*-type germanium is mentioned.

2917: M. P. Rappoldt: Studies on vitamin D and related compounds, XIV; investigations on sterols, XVII. The photoisomerization of pre-ergocalciferol and tachysterol$_2$ (Rec. Trav. chim. Pays-Bas **79**, 1012-1021, 1960, No. 9/10).

The quantum yields of the isomerization reactions of pre-ergocalciferol (P) and tachysterol$_2$ (T) in ether at 20 °C under the influence of ultraviolet light of 2537 Å were found to be 0.49 and 0.11 respectively. It had previously been found that irradiation of P gives rise to small quantities of ergosterol (E) and lumisterol$_2$ (L). It is now shown that E is formed directly from P, but not from T, while L is probably formed from T produced by the isomerization of P.

A 32: H. G. Grimmeiss, W. Kischio and A. Rabenau: Über das AlP; Darstellung, elektrische und optische Eigenschaften (Phys. Chem. Solids **16**, 302-309, 1960, No. 3/4). (Preparation and electrical and optical properties of AlP; in German.)

Methods of preparing and doping AlP are described. Reflectivity and transmission measurements indicate that the band gap of this compound is 2.42 eV at 20 °C. Undoped crystals show electroluminescence with maxima at 5550 and 6150 Å. This effect is shown to be due to the recombination of charge carriers injected from *P-N* junctions. The maximum photoluminescence is found at 6100 Å. These results together with conductivity data allow the band structure of undoped AlP to be deduced. AlP crystals also show point-contact rectification and photovoltaic effects. The maximum photoconductivity is found between 5000 and 5150 Å.

A 33: A. Stegherr, F. Wald and P. Eckerlin: Über eine ternäre Phase im System Ag-Sb-Te (Z. Naturf. **16a**, 130-131, 1961, No. 1). (A ternary phase in the system Ag-Sb-Te; in German.)

A ternary phase with the NaCl structure found in the system Ag-Sb-Te is briefly described. The homogeneity range varies considerably with temperature, but it is obvious that this phase cannot be described as "the compound $AgSbTe_2$", as other workers have done. The composition $Ag_{19}Sb_{29}Te_{52}$ seems much nearer the truth. This corresponds very nearly to the formula $2\ Ag_2Te.3\ Sb_2Te_3$; the crystallographic formula can be written $Ag_{0.366}Sb_{0.558}\square_{0.077}Te$.

A 34: A. Rabenau and P. Eckerlin: Compounds in the system Be_3N_2-Si_3N_4 (Special Ceramics, Proc. Symp. Brit. Ceramic Res. Ass., Ed. P. Popper, pp. 136-143, Heywood, London 1960).

The preparation of the substances mentioned in this article requires a special technique which is described and which has a wide range of applications to other investigations. The system Be_3N_2-Si_3N_4 was investigated between 1600 and 2000 °C. There exists a new hexagonal modification of Be_3N_2 which dissolves up to 7 mol. per cent Si_3N_4. Further compounds in the system are Be_4SiN_4 and the wurtzite-type compound $BeSiN_2$.

A 35: R. Groth: Über Ultrarotempfänger auf der Basis von Phosphoren (Z. Naturf. **16a**, 169-172, 1961, No. 2). (Infrared detectors based on phosphors; in German.)

An infrared detector based on infrared-sensitive phosphors is proposed. The principle of such a detector is explained, and experimental data obtained with a SrS-Ce-Sm phosphor are given. It was possible to obtain a sensitivity of 6×10^{-11} W with this phosphor, for wavelengths around 1 micron.

A 36: I. Maak, P. Eckerlin and A. Rabenau: Über $GaF_3.3H_2O$ und andere Trifluoridtrihydrate (Naturwiss. **48**, 218, 1961, No. 7). ($GaF_3.3H_2O$ and other trifluoride-trihydrates; in German.)

A preliminary report of an investigation of the structure of $GaF_3.3H_2O$. This compound gives the same X-ray powder diffraction pattern as α-$AlF_3.3H_2O$, and forms mixed crystals with the latter in all proportions. The lattice constants of $GaF_3.3H_2O$ and of other compounds isomorphous with α-$AlF_3.3H_2O$ and with β-$AlF_3.3H_2O$ are given.

A 37: K. Weiss, P. Fielding and F. A. Kröger: Untersuchungen an kupferdotiertem Wismuttellurid Bi_2Te_3 (Z. phys. Chem. Neue Folge (Frankfurt a.M.) **26**, 145-158, 1960, No. 3/4). (Investigations on copper-doped bismuth telluride; in German.)

An investigation of the influence of copper on the electrical and mechanical properties of P-Bi_2Te_3. The experimental results cannot be satisfactorily explained on the assumption that all the copper occupies interstitial sites. The behaviour of the dissolved copper can better be understood if the layer structure of Bi_2Te_3 and the resulting anisotropy of the host lattice are taken into account.

A 38: A. Klopfer and W. Schmidt: An omegatron mass spectrometer and its characteristics (Vacuum **10**, 363-372, 1960, No. 5).

An omegatron with noble-metal electrodes is described, which can be given a constant sensitivity to within 10 per cent by the application of a suitable electrostatic field. The sensitivity is not even affected by the action of gases and vapours, such as H_2O, CO_2 and CH_4, over long periods, and is reproducible from omegatron to omegatron as long as the dimensions are kept constant. A comparison of the ionization probability given in the literature with that calculated from the calibration curve of the omegatron shows that nearly all the resonance ions formed by the electron beam reach the ion collector. The adjustment of the operating data needed to achieve this condition is in general independent of the mass. Some characteristics of the omegatron are described. (See also Philips tech. Rev. **22**, 195, 1960/61 (No. 6) and **23**, 122, 1961/62 (No. 4).)

A 39: G. Schuchhardt: Ion movements in an omegatron (Vacuum **10**, 373-376, 1960, No. 5).

The motion of resonant and non-resonant ions in the omegatron described in **A 38** is investigated. It is shown that the auxiliary electrostatic field in this type of omegatron creates conditions which make for optimum collection of the resonant ions and ensure reproducible results. Space-charge effects are estimated, and an expression is derived for the resolving power.